

2020

## A Computational Analysis of Marine Fenders Under Heavy Weather Mooring Conditions

Zachary Eskew

University of North Florida, n01438972@unf.edu

Follow this and additional works at: <https://digitalcommons.unf.edu/etd>



Part of the [Other Civil and Environmental Engineering Commons](#)

---

### Suggested Citation

Eskew, Zachary, "A Computational Analysis of Marine Fenders Under Heavy Weather Mooring Conditions" (2020). *UNF Graduate Theses and Dissertations*. 997.

<https://digitalcommons.unf.edu/etd/997>

This Master's Thesis is brought to you for free and open access by the Student Scholarship at UNF Digital Commons. It has been accepted for inclusion in UNF Graduate Theses and Dissertations by an authorized administrator of UNF Digital Commons. For more information, please contact [Digital Projects](#).

© 2020 All Rights Reserved

A COMPUTATIONAL ANALYSIS OF MARINE FENDERS UNDER HEAVY WEATHER  
MOORING CONDITIONS

By

ZACHARY BRIAN ESKEW

A THESIS PRESENTED TO THE GRADUATE SCHOOL  
OF THE UNIVERSITY OF NORTH FLORIDA IN PARTIAL FULFILLMENT  
OF THE REQUIREMENTS FOR THE DEGREE OF  
MASTER OF SCIENCE IN CIVIL ENGINEERING

UNIVERSITY OF NORTH FLORIDA

2020

This thesis titled “A Computational Analysis of Marine Fenders under Heavy Weather Mooring Conditions” written by Zachary Brian Eskew has been approved by:

---

Raphael Crowley, PhD PE

---

Donald Resio, PhD

---

Adel ElSafty, PhD, PE

Accepted for the School of Engineering:

---

Osama Jadaan, PhD  
Director of the School of Engineering

Accepted for the College of Computing, Engineering, and Construction:

---

William Klostermeyer, PhD  
Dean of Engineering

Accepted for the University:

---

John Kantner, PhD RPA  
Dean of the Graduate School

© 2020 Zachary Eskew

To my Wife, Kiera.

## ACKNOWLEDGMENTS

I would like to thank my thesis advisor, Dr. Raphael Crowley, for all of his assistance with this project, especially during the complete retooling of our plan during the coronavirus pandemic. I could not have completed this project without his guidance.

I would also like to thank Mr. Eric Sites of NAFVAC EXWC, Mr. John McCoy and Mr. Eric Cannon of NAVFAC Southeast, and Mr. Robert Dove of Trelleborg, for their assistance, they were instrumental in the completion of this thesis.

# TABLE OF CONTENTS

	<u>page</u>
ACKNOWLEDGMENTS .....	5
TABLE OF CONTENTS .....	6
LIST OF TABLES .....	8
LIST OF FIGURES .....	9
INTRODUCTION AND BACKGROUND.....	14
1.1 Importance of Dynamic Loading of Marine Fenders .....	14
1.2 Industry Testing Standards .....	15
1.3 United States Navy Standards .....	16
1.3.1 TR-6015-OCN Foam Filled Fender Design to Prevent Hull Damage (NFESC, 1997).....	16
1.3.2 UFC 4-152-01 Design: Piers and Wharves (DoD, 2017) .....	17
1.3.3 UFC 4-159-03 Design: Moorings (DoD, 2020) .....	18
1.4 Heavy Weather Mooring Analysis .....	19
1.5 Fenders Used by USN .....	22
1.6 Goals and Objectives .....	23
1.7 Thesis Organization .....	24
METHODOLOGY .....	25
2.1 Finite Element Analysis (FEA) Model.....	25
2.2.1 Reference Frame .....	26
2.2.2 Governing Equations.....	26
2.2.3 Time Integration .....	27
2.2 Material Properties.....	28
2.2.1 Fender Properties.....	28
2.2.2 Ship and Caisson Properties .....	31
2.3 Boundary Conditions.....	32
2.4 Mesh Characteristics .....	35
2.5 Testing Methods .....	36
2.5.1 Quasi-Static Testing .....	36
2.5.2 Cyclic Velocity Testing.....	37
2.6 Data Analysis .....	40
RESULTS.....	41
3.1 Quasi-Static Testing.....	41
3.2 Cyclic Testing .....	45

DISCUSSION .....	52
4.1 Quasi-Static Testing.....	52
4.2 Cyclic Testing .....	54
4.3 Conclusions .....	55
LIST OF REFERENCES .....	60
BIOGRAPHICAL SKETCH.....	61



## LIST OF TABLES

<u>Table</u>	<u>page</u>
Table 2-1. Performance data for Trelleborg SeaGuard 7 ft by 14 ft fender (Trelleborg Marine Systems, 2018). .....	28
Table 2-2. Trelleborg material properties for SeaGuard fender skin. (Trelleborg Marine Systems, 2018).....	29
Table 2-3 Trelleborg material properties for SeaGuard fender core. (Trelleborg Marine Systems, 2016).....	30
Table 2-4. Model material properties for fender skin. ....	30
Table 2-7. Model properties for pier wall/caisson. ....	32
Table 2-8. Static testing velocity testing matrix .....	37
Table 2-9. Cyclic velocity testing matrix. ....	39

## LIST OF FIGURES

<u>Figure</u>	<u>page</u>
Figure 1-1. Graph depicting the hull pressure exerted by SEA-GUARD fenders of various sizes, as well as the corresponding fender percent compression. (DoD, 2020).....	19
Figure 1-3. Overview of USN Heavy Weather Mooring testing profile.....	20
Figure 1-4. Chart of forces exerted on each fender during the three-hour testing period versus frequency. Note: there are only four fenders listed as they were the only 4 to record a reading during the test. ....	21
Figure 1-5. Chart of percent of maximum rated deflection on each fender during the three-hour testing period versus frequency. Note: there are only four fenders listed as they were the only 4 to record a reading during the test.....	22
Figure 1-6. Example construction diagram of a Trelleborg Seaguard marine fender (Trelleborg, 2017).....	23
Figure 2-1. Problem time magnitude versus nonlinearity (adapted from <a href="http://www.mechead.com/what-is-explicit-dynamics-in-ansys/">http://www.mechead.com/what-is-explicit-dynamics-in-ansys/</a> ).....	25
Figure 2-2. Fender dimensions. ....	28
Figure 2-3. Generic plot for SeaGuard fender reaction and energy as a function of fender deflection. (Trelleborg Marine and Infrastructure, 2017).....	29
Table 2-5. Model properties for fender core. ....	31
Figure 2-4. Isometric view of fender testing model, with fender width and radius. ....	32
Figure 2-5. View of fender with fixed support on pier highlighted in blue.....	33
Figure 2-8. View of fender testing model with mesh visible.....	36
Figure 2-9. Plot of ship velocity as it pertains to ship weight and berthing conditions as seen in UFC 4-152-01 (DoD, 2017).....	38
Figure 2-10. Example velocity profile for cyclic testing. X-axis has units of seconds, and Y-axis has units of m/s. ....	39
Figure 3-1. Quasi-static simulation with 2 m/s ship velocity results.....	42
Figure 3-2. Quasi-static simulation with 1 m/s ship velocity results.....	42
Figure 3-3. Quasi-Static simulation with 0.5 m/s ship velocity results .....	43

Figure 3-4. Quasi-static simulation with 0.25 m/s ship velocity results .....	43
Figure 3-5. Quasi-static simulation with 0.125 m/s ship velocity results .....	44
Figure 3-6. Quasi-static simulation with 0.0625 m/s ship velocity results .....	44
Figure 3-7. Cyclic test with 0.15 m/s ship velocity and 1.5 s period results .....	45
Figure 3-8. Cyclic test with 0.25 m/s ship velocity and 1.5 s period results .....	46
Figure 3-9. Cyclic test with 0.334 m/s ship velocity and 1.5 s period results .....	46
Figure 3-10. Cyclic test with 0.15 m/s ship velocity and 3 s period results .....	47
Figure 3-11. Cyclic test with 0.25 m/s ship velocity and 3 s period results .....	47
Figure 3-12. Cyclic test with 0.334 m/s ship velocity and 3 s period results .....	48
Figure 3-13. Cyclic test with 0.15 m/s ship velocity and 4.5 s period results .....	48
Figure 3-14. Cyclic test with 0.25 m/s ship velocity and 4.5 s period results .....	49
Figure 3-15. Cyclic test with 0.334 m/s ship velocity and 4.5 s period results .....	49
Figure 3-16. Cyclic test with 0.15 m/s ship velocity and 6 s period results .....	50
Figure 3-17. Cyclic test with 0.25 m/s ship velocity and 6 s period results .....	50
Figure 3-18. Cyclic test with 0.334 m/s ship velocity and 6 s period results .....	51
Figure 4-1. Plot of all quasi-static testing simulations with line of best fit and equation.....	52
Figure 4-2. Plot of percent of maximum deflection of the fender at failure as a function of loading speed.....	53
Figure 4-3. LDPE foam core of fender at failure during 2 m/s quasi-static testing.....	54
Figure 4-4. Plot of all cyclic testing simulations with line of best fit and equation. ....	55
Figure 4-5. Compiled plots of both cyclic and quasi-static testing, along with their lines of best fit.....	56
Figure 4-6. Starting position of cyclic testing simulation, with the ship model in contact with the fender model.....	57
Figure 4-7. Cyclic testing simulation at time $T/4$ , at full compression. ....	57

Figure 4-8. Cyclic testing simulation at time $3T/4$ , at its farthest position from the fender. ....	58
---	----

Abstract of Thesis Presented to the Graduate School  
of the University of North Florida in Partial Fulfillment of the  
Requirements for the Degree of Master of Science in Civil Engineering

A COMPUTATIONAL ANALYSIS OF MARINE FENDERS UNDER HEAVY WEATHER  
MOORING CONDITIONS

By

Zachary Brian Eskew

December 2020

Chair: Raphael Crowley, PE  
Major: Civil Engineering

Dynamic loading of marine fenders is a situation that is unique to the United States Navy (USN), due to the use of Heavy Weather Mooring (HWM) for naval vessels during extreme weather events, such as hurricanes. Traditional analysis has not been concerned with the fender reaction on vessel hulls. However, newer classes of Naval ships, such as the Littoral Combat Ships (LCS), have designs that emphasize speed and agility, resulting in them having thinner hulls more susceptible to damage from fenders. In traditional analysis, fenders are modeled as idealized springs, with static-load derived spring constants from manufacturer charts. This has been adequate for previous warships, however with more susceptible warships, a better understanding of the fenders reaction is required.

Two series of tests were created, a quasi-static testing series to mimic the current testing of fenders, and a cyclic testing series to determine if repeated loading of fenders would provoke a dynamic response.

Testing was conducting using a Finite Element Analysis (FEA) model to simulate ship impacts on fenders and determine the fender reaction to both quasi-static and cyclic loading patterns at various ship velocities and loading periods.

This research found that there was no impact on fender response provoked by a difference in loading speed during quasi-static testing. Cyclic loading of the fender did not provoke a dynamic fender response even under a second wave cycle where impact forcing could have caused different behavior. Overall, results of this study lead to the conclusions that both loading speed and loading pattern do not have an impact on fender response.

## CHAPTER 1 INTRODUCTION AND BACKGROUND

### **1.1 Importance of Dynamic Loading of Marine Fenders**

The issue of dynamic loading of marine fenders is a situation that is unique to the United States Navy (USN). This uniqueness derives from another condition unique to the USN, Heavy Weather Mooring (HWM). Heavy Weather Mooring is the condition in which Naval vessels stay in port during extreme weather events, such as tropical storms and hurricanes. Traditionally, most vessels would leave port to avoid the worst impacts of these storms. However, according to OPNAV INST 4700.7M Maintenance Policy for Navy Ships (2019), Naval vessels are routinely placed in conditions that prevent them from leaving port for periods of at least 6 months, up to multiple years, during which they are undergoing extensive repairs and upgrades. These situations necessitate the need for Heavy Weather Mooring.

Traditional analysis of Heavy Weather Mooring conditions on vessels has not been concerned with the fender reaction on vessel hulls. This was due to the robust nature of traditional Naval ships, which were impervious to damage from the fenders. However, newer classes of Naval ships, such as the Littoral Combat Ships (LCS), have designs that emphasize speed and agility, resulting in them having thinner hulls. This tradeoff has resulted in the newer ships being more susceptible to damage from fenders during Heavy Weather Mooring events.

In traditional Heavy Weather Mooring analysis, fenders are modeled as idealized springs, with spring constants derived from manufacturer provided load versus deflection charts. These charts, however, are for a static loading case. In the past, this has not been an issue, due to the previously stated robust nature of warships. However,

with the newer, more susceptible warships, a better understanding of the fenders reaction under dynamic conditions is required.

## 1.2 Industry Testing Standards

The current industry standard for the testing of marine fenders is ASTM F2192-05, Standard Test Method for Determining and Reporting the Berthing Energy and Reaction of Marine Fenders. This method covers foam filled fenders, as well as rubber and pneumatic fenders. As stated by ASTM, “Its primary purpose is to ensure that engineering data reported in manufacturers’ catalogues are based upon common testing methods.” For testing ASTM allows for two methods. The first method calls for a constantly decreasing velocity, with the velocity determined through the use of either equation 1-1 or 1-2.

$$V = \frac{V_0(D - d)}{D} \text{ or } 0.005 \frac{m}{s} \text{ whichever is greater} \quad (1-1)$$

$$V = V_0 \sqrt{\frac{E - e}{E}} \text{ or } 0.005 \frac{m}{s} \text{ whichever is greater} \quad (1-2)$$

Where  $V_0$  is the initial deflection velocity,  $D$  is the rated deflection of the fender,  $d$  is the instantaneous deflection of the fender,  $E$  is the rated energy absorption of the fender, and  $e$  is the instantaneous running total of energy absorbed. The second method calls for the fender to be deflected at a constant velocity of 0.15 m/s to the rated deflection of the fender.



Both of these methods call for the fender to be “broken in” before the initial testing, with a minimum recovery time before testing of one hour. This testing method is adequate for manufacturers’ data, but they provide no data in terms of dynamic loading of the fender, as the rated data is taken from a single compression of the fender.

### **1.3 United States Navy Standards**

The United States Navy does not have a single specific document regulating the construction and use of foam filled fenders; instead, this topic is addressed in multiple sources. Two of the documents, Unified Facilities Criteria (UFC) 4-152-01 (DoD, 2017), and UFC 4-159-03 (DoD, 2020), are documents issued by the Department of Defense that provide guidance and standards for all military construction. The other main document TR-6015-OCN (NFESC, 1997), was published by Naval Facilities Engineering Command. These documents are used in the proper sizing and use of foam fenders in the USN

#### **1.3.1 TR-6015-OCN Foam Filled Fender Design to Prevent Hull Damage (NFESC, 1997)**

This report covers, as the title suggests, the design of foam filled fenders to prevent hull damage. However, this report was published in 1997, and has not been updated since. In the report, it specifically states that, “This report examines only carbon steel hulls fabricated from grades of steel varying from 34 ksi yield to 100 ksi yield” (NFESC, 1997). As such, this report, which is partially the basis for the following two design manual fender sections, is not applicable to LCS hulls, as they are not composed of carbon steel. This report mostly addresses the stresses that would be exerted on the ship, such as the yielding and bending stresses that would be allowed for different ships in different situations (DoD, 1997). The report does not take into

consideration specific fender properties, except for in section 6 Foam filled fender characteristics., where it is stated that,

Cross—linked foam composes the core of most foam-filled fenders. The foam deforms elastically when subjected to an applied force. The relationship between pressure and deflection is non-linear, due in part to the shape of the fender. See Attachment A.<sup>xvi</sup> To prevent damage to the fender, manufacturers normally recommend that the fender not exceed 60% compression under design conditions. At this deflection, most fenders exhibit a reactive pressure of approximately 25 psi. (NFESC, 1997)

The document referenced as Attachment A is the Sea Cushion Design Manual, published in 1982 by Seaward International, Inc. This document was not able to be located.

This report seems to be more to provide guidance to the fender manufacturers on the requirements that their fenders need to meet, rather than a serious analysis on the characteristics of foam filled fenders. It does not have any data on fender reactions and no data on possible fender dynamic responses.

### **1.3.2 UFC 4-152-01 Design: Piers and Wharves (DoD, 2017)**

Unified Facilities Criteria 4-152-01 Design: Piers and Wharves, which is issued by the United States Department of Defense, and governs the Department of the Navy, includes in it Chapter 5, Fender Systems, that covers the considerations and selection of fender systems for naval vessels (DoD, 2017). This document, and Chapter 5 specifically, addresses all fender systems used by the United States Government, and as such is not exclusively focused on floating foam fenders. The document's chapter on the design of fender systems mostly addresses the proper dissipation of berthing and mooring energy transmitted from the ship to the fender system. The only guidance in reference to hull damage is in section 5-4.1.3. Hull Pressure, which states:

This is the pressure exerted on the ship's hull by the fender unit and is derived by dividing the reaction force by the fender area in contact with the ship. Limit hull pressure to levels that will not cause permanent damage to the berthing ship. (DoD, 2017)

And, Section 5-4.4.2. Allowable Hull Pressure states:

When the ship's energy is resisted through foam-filled or pneumatic fenders, the resulting force is concentrated in a small area of the ship's hull. In such cases, the allowable pressure on the ship's hull becomes a critical design issue. Most surface combatants have a thin hull plating with a low allowable pressure. For more specific information on the ships being berthed, consult NAVSEA. See TR-6015-OCN *Foam Filled Fender Design to Prevent Hull Damage*, and note that the values in Table 7 are based on yielding of the hull plating and include a 1.5 safety factor. Consequently, when checking for an accidental condition, the allowable value for hull pressure may be increased by up to 50 percent. (DoD, 2017)

As seen in section 1.3.1, TR-6015-OCN does not specifically address the fender response beyond giving upper limits for different ships. As with TR-6015-OCN, UFC 4-152-01 seems to be more of a guidance document for fender manufacturers' than an analysis of fender reactions.

### **1.3.3 UFC 4-159-03 Design: Moorings (DoD, 2020)**

Unified Facilities Criteria 4-159-03 Design: Moorings is issued by the United States Department of Defense and governs the Department of the Navy. Included in this document are Chapter 6, Facility Mooring Equipment Guidelines, and paragraph 6.1, Fenders. Like UFC 4-152-01, UFC 4-159-03 refers all detailed fender questions to TR-6015-OCN. It does however contain a chart, shown in Figure 1-1, detailing the hull pressures exerted by different sized Sea-Guard fenders at different compression levels and the forces required at each compression level (DoD, 2020). However, while no information is given on how this data was collected, it can be assumed that the fender information given was determined using the traditional static loading method.

Figure 6-3. SEA-GUARD Fender Information

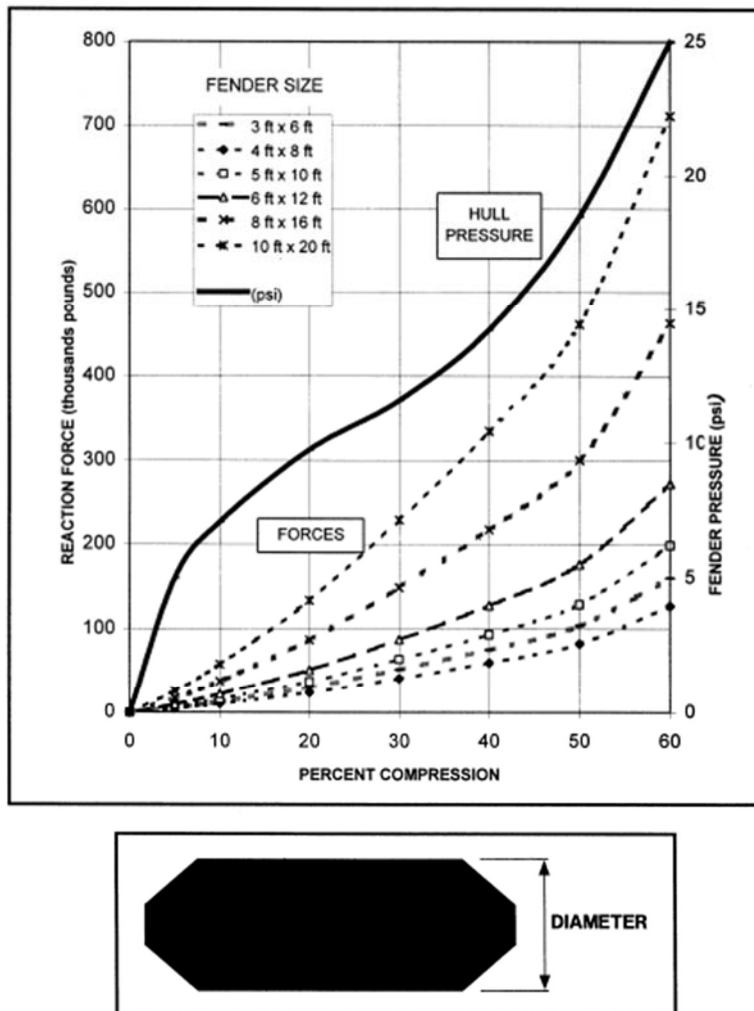


Figure 1-1. Graph depicting the hull pressure exerted by SEA-GUARD fenders of various sizes, as well as the corresponding fender percent compression. (DoD, 2020)

While this data is helpful, UFC 4-159-03, like TR-6015-OCN and UFC 4-152-01, seem to be more of guidance documents than an analysis of fender performance.

#### 1.4 Heavy Weather Mooring Analysis

As stated previously, analysis of Heavy Weather Mooring conditions has not traditionally been concerned with fender reactions on the hulls of the warships.

The current testing, conducted by NAVFAC EXWC, uses the AQWA module of ANSYS. Data from a testing run was provided by the USN. In this testing run, a vessel was moored alongside a wharf under HWM conditions. The wind was defined by the Ochi Shin spectrum, with a 30-second wind speed of 80 knots and 1-hour wind speed of 57 knots, at a direction of 270 degrees. The significant wave height,  $H_s$ , was 3.3 feet. The significant wave period,  $T_z$ , was 5 seconds. The waves were modeled using a Pierson-Moskowitz spectrum, at a direction of 270 degrees, perpendicular to the ship. In terms of the model, shown in Figure 1-3, the waves travelled along the y-axis.

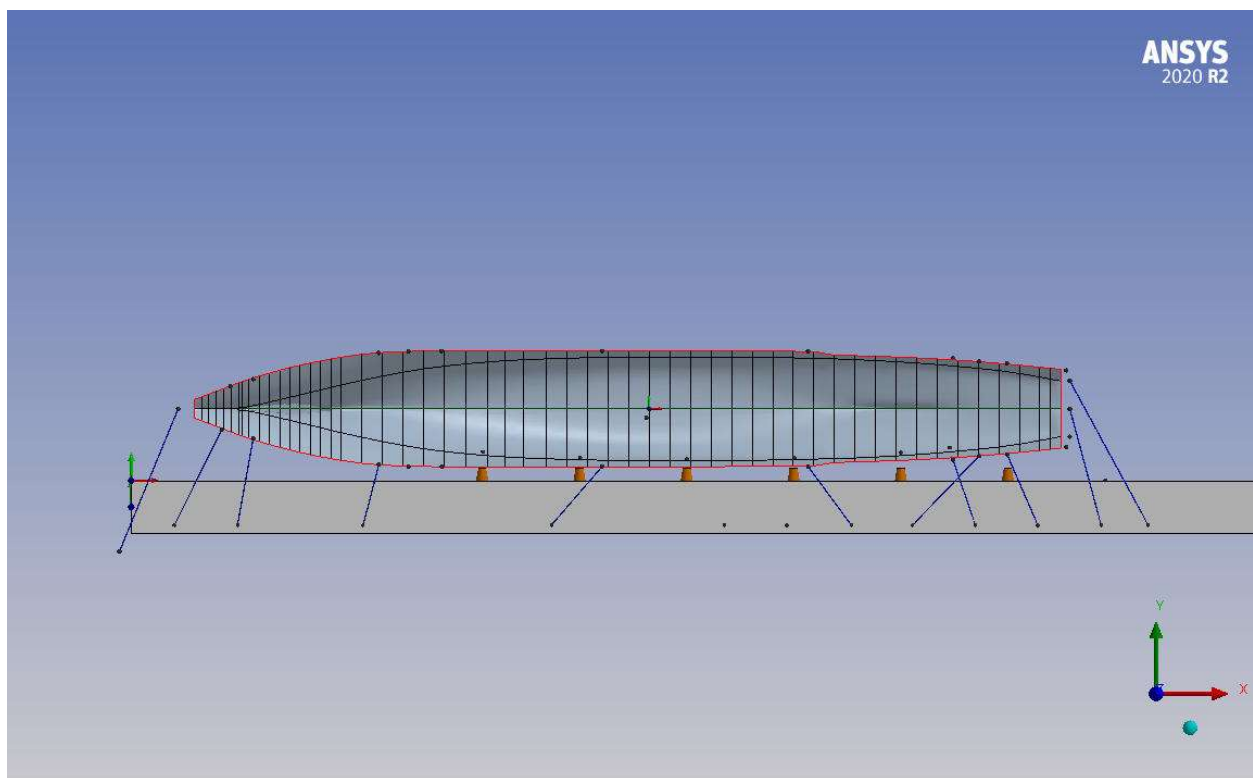


Figure 1-3. Overview of USN Heavy Weather Mooring testing profile.

The fenders were idealized as single springs, with a spring coefficient of 0.9 s, derived from the manufacturer published, static load testing determined fender capabilities. These tests are used to produce loads on the fender, which are useful in

the determining if the fender will fail but not useful in determining the fender reaction on the ship. Forcing upon the ship hull associated with these events at each fender (assuming springs) is shown below in Fig. 1-3 and Fig. 1-4:

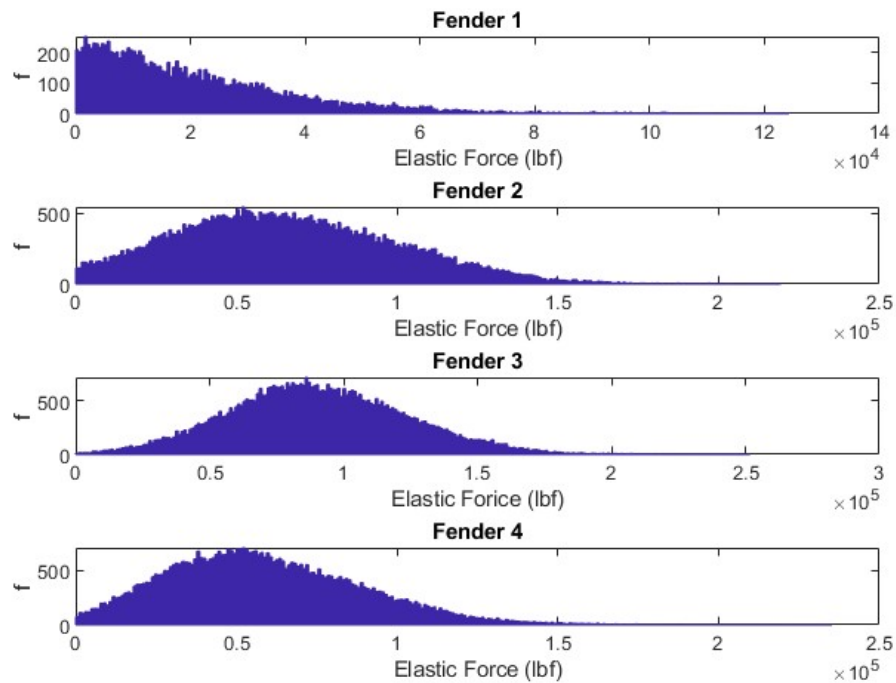


Figure 1-4. Chart of forces exerted on each fender during the three-hour testing period versus frequency. Note: there are only four fenders listed as they were the only 4 to record a reading during the test.

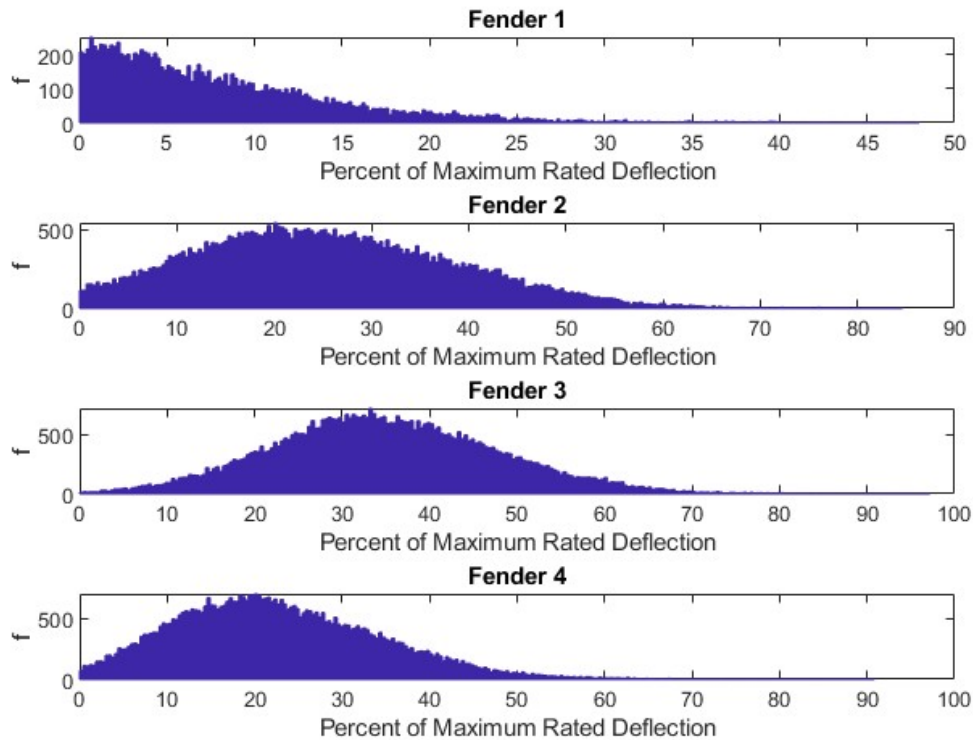


Figure 1-5. Chart of percent of maximum rated deflection on each fender during the three-hour testing period versus frequency. Note: there are only four fenders listed as they were the only 4 to record a reading during the test.

This testing provided valuable information on the possible loads and frequency of impacts that fenders undergo during a HWM event. However, due to the fact that the fenders themselves were modelled as idealized springs with damping coefficients derived from the static testing data, there is no information to be derived from it about possible dynamic responses of fenders. In other words, these data depend upon the assumption that the dynamic load response of fenders is similar to fenders' static load responses. It is unclear if this is actually the case.

### 1.5 Fenders Used by USN

The United States Navy mostly uses floating foam fenders for the mooring of naval vessels. For the purposes of this thesis, the focus of the analysis will be on the

Trelleborg SeaGuard Foam Filled Fender, a commonly used fender by the United States Navy (see Fig. 1-5 below).

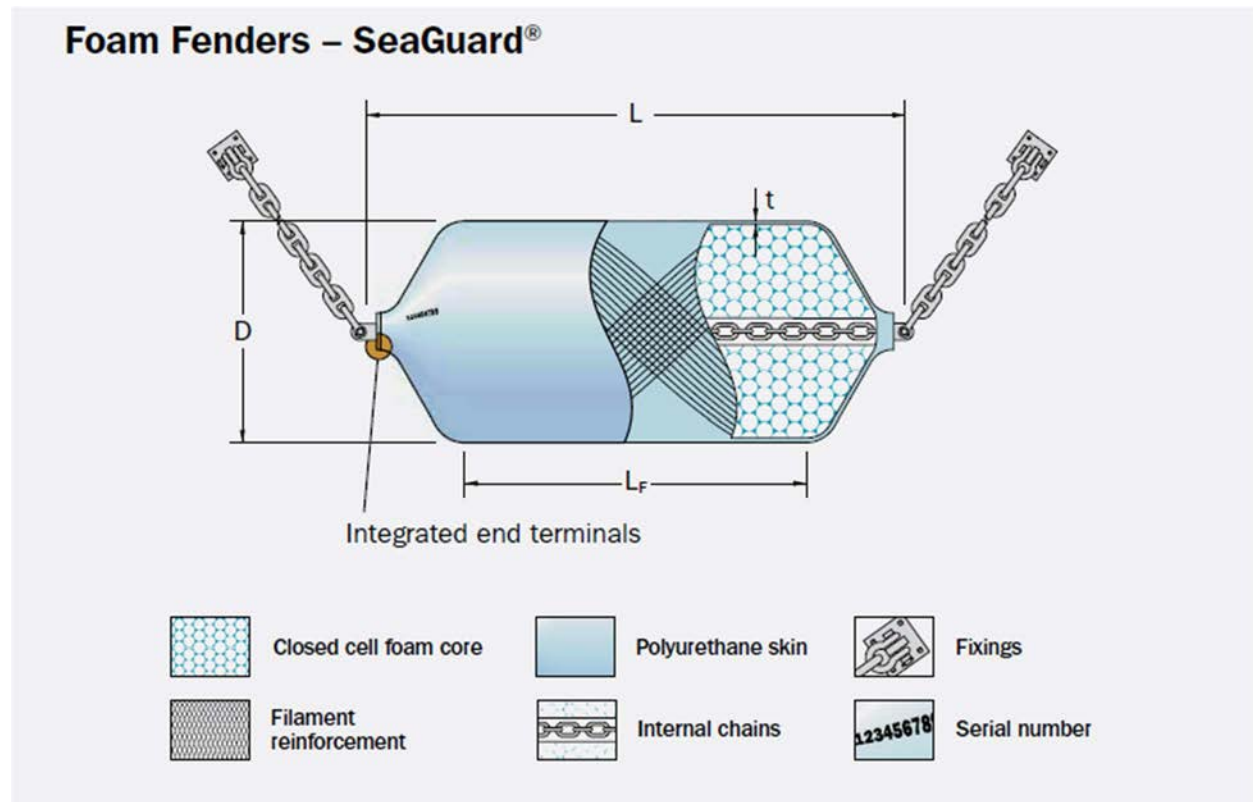


Figure 1-6. Example construction diagram of a Trelleborg Seaguard marine fender (Trelleborg, 2017)

This type of fender utilizes a closed-cell polyethylene foam core and an outer skin of reinforced polyurethane elastomer. These fenders dissipate the forces from the ships impact through their physical deformation. More detailed information on the specific fender properties can be found in chapter 2, methodology.

## 1.6 Goals and Objectives

The goal of this thesis is to determine the response of marine fenders in a dynamic loading situation. Specifically, this thesis attempts to address if fender dynamic load response is significantly different from static load response. And, if dynamics load response is significantly different, an ancillary goal is to quantify these differences. This



was initially planned to be accomplished through physical testing of fenders under dynamic loading conditions. However, due to the COVID-19 pandemic, this was not achievable in the timeframe of this thesis. As a first cut at answering this question then, computational simulations were used instead to model the fenders and their reaction to dynamic loading. Then, these data were analyzed using the same methods that would have been used with physical fender data.

### **1.7 Thesis Organization**

This thesis is organized into five chapters:

- Chapter one presented the background information on the importance of dynamic loading of fenders and a review of relevant literature and USN documentation on marine fenders and their application
- Chapter two presents the methodology used in the execution of this thesis, including the equations used by the modelling software
- Chapter three presents the results of the computer modelling
- Chapter four presents the discussion of the results shown in chapter four
- Chapter five presents a summary, preliminary conclusions, and recommendations for future work.

## CHAPTER 2 METHODOLOGY

### 2.1 Finite Element Analysis (FEA) Model

ANSYS Workbench 2020 R1 was used throughout this study. Specifically, its explicit dynamics finite element (FE) model was utilized. Figure 2-1 below shows an approximate relationship between problem timescale magnitude and expected nonlinearity:

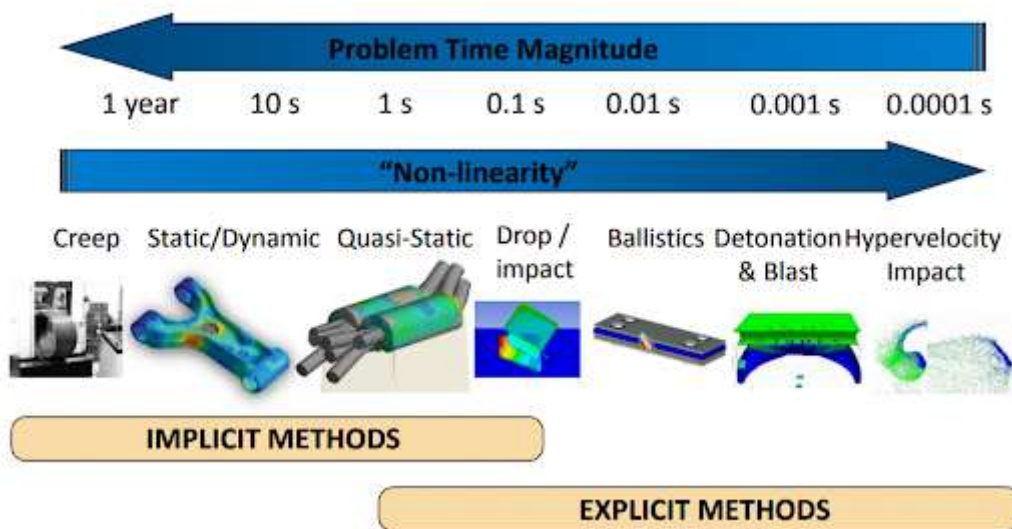


Figure 2-1. Problem time magnitude versus nonlinearity (adapted from <http://www.mechead.com/what-is-explicit-dynamics-in-ansys/>)

In the case of ship fender impacts, one would expect the governing timescales to be on the order of hundredths of a second, (when the ship first strikes the fender), to tens of seconds, (as would be seen with typical wave periods). As such, this fender/structure/ship interaction problem spans both implicit and explicit timescales. In these sorts of situations, the appropriate solution is to err on the side of the smaller timescales. As such, the explicit solver (as opposed to an implicit transient solver, which would only be appropriate for deflection timescales in tens of seconds) appeared to be

appropriate. Details associated with the selected explicit dynamics model are presented in this section.

### 2.2.1 Reference Frame

The ANSYS explicit dynamics model utilizes a Lagrangian reference frame. As such, a mesh is created that is fitted to the body or bodies being analyzed. This mesh is divided into elements, and each element is assigned a specific volume and mass of the body material. This assigned mass remains associated with each element throughout the simulation. As the mesh deforms throughout the simulation, the mass deforms as well.

### 2.2.2 Governing Equations

Like most FE structural models, the ANSYS explicit structural dynamics model conserves mass. As the model is run at each timestep, the model's mesh deforms and distorts as the material distorts. Eq. 2-1 is used to determine an element's density at any given timestep:

$$\frac{\rho_0 V_0}{V} = \frac{m}{V} \quad (2-1)$$

where  $\rho_0$  is the initial density of the zone,  $V_0$  is the initial volume,  $m$  is the current mass of the zone, and  $V$  is the current volume of the zone.

In addition, conservation of momentum is enforced. The governing momentum equations are presented below in Eq. 2-2 through Eq. 2-4

$$\rho \ddot{x} = b_x + \frac{d\sigma_{xx}}{dx} + \frac{d\sigma_{xy}}{dy} + \frac{d\sigma_{xz}}{dz} \quad (2-2)$$

$$\rho \ddot{z} = b_z + \frac{d\sigma_{zx}}{dx} + \frac{d\sigma_{zy}}{dy} + \frac{d\sigma_{zz}}{dz} \quad (2-3)$$

$$\rho \ddot{y} = b_y + \frac{d\sigma_{yx}}{dx} + \frac{d\sigma_{yy}}{dy} + \frac{d\sigma_{yz}}{dz} \quad (2-4)$$

Where  $b_i$  is the body force in the x, y, or z direction,  $\rho$  is the material density, and  $\sigma_{ij}$  is the stress tensor. Finally, energy is conserved via Eq. 2-5:

$$\dot{e} = \frac{1}{\rho} (\sigma_{xx}\dot{\epsilon}_{xx} + \sigma_{yy}\dot{\epsilon}_{yy} + \sigma_{zz}\dot{\epsilon}_{zz} + 2\sigma_{xy}\dot{\epsilon}_{xy} + 2\sigma_{yz}\dot{\epsilon}_{yz} + 2\sigma_{zx}\dot{\epsilon}_{zx}) \quad (2-5)$$

where  $\dot{e}$  is the work done,  $\rho$  is the material density,  $\sigma_{ij}$  is the stress tensor, and  $\dot{\epsilon}_{ij}$  is the strain tensor.

For all of these equations, explicit solutions are determined for each element in the model, based on the previous timestep input values. It is important to note that equilibrium is not required for an explicit dynamics solution by the solver.

### 2.2.3 Time Integration

ANSYS' explicit dynamics solver uses central differencing time integration to compute each element's acceleration according to Eq. 2-6:

$$\ddot{x}_i = \frac{F_i}{m} + b_i \quad (2-6)$$

where  $\ddot{x}_i$  are the components of nodal acceleration,  $F_i$  are the forces acting on the nodal points,  $b_i$  are the components of body acceleration, and  $m$  is the mass attributed to the node. These accelerations are then used to determine the velocities and positions of each node in the mesh, using equations 2-7 and 2-8, respectively.

$$\dot{x}_i^{n+1/2} = \dot{x}_i^{n-1/2} + \ddot{x}_i^n \Delta t^n \quad (2-7)$$

$$x_i^{n+1} = x_i^n + \dot{x}_i^{n+1/2} \Delta t^{n+1/2} \quad (2-8)$$

Where  $x_i$  are the components of nodal positions,  $\dot{x}_i$  are the components of nodal velocity, and  $\ddot{x}_i$  are the components of nodal acceleration.

## 2.2 Material Properties

### 2.2.1 Fender Properties

As discussed in Section 1.5, this study focused on the Trelleborg SeaGuard foam filled marine fender. These fenders come in a variety of different loading and reaction varieties, including standard, high, extra high, and super high capacity fenders, as well as low reaction fenders (Trelleborg, 2017). For this thesis, the standard capacity fender was analyzed, because it is the most common fender used by the United States Navy. Figure 2-2 shows the fender's dimensions while its properties are presented in Table 2-1:

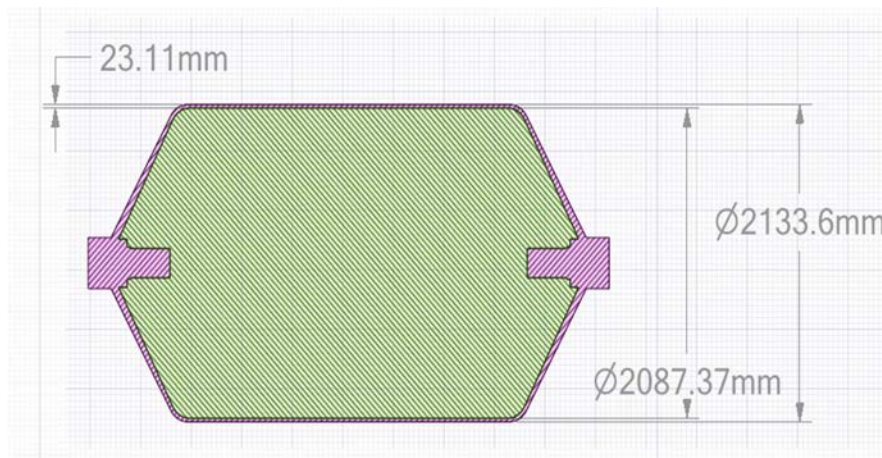


Figure 2-2. Fender dimensions.

Table 2-1. Performance data for Trelleborg SeaGuard 7 ft by 14 ft fender (Trelleborg Marine Systems, 2018).

Size: 7 ft x 14 ft	English Units	SI Units	Metric Units
Performance at 60 % Compression			
Energy Absorption	487 ft-kip	660 kN-m	67.3 ton-m
Reaction Force	259 kip	1152 kN	117.5 ton
Average Reaction Pressure	3.3 kip/ft <sup>2</sup>	155 kPa	15.9 ton/m <sup>2</sup>

The reaction/deflection curve associated with this fender is shown below in Fig. 2-3 (Trelleborg Marine and Infrastructure, 2017). In addition, the individual material properties for the fender materials – i.e., the polyurethane skin and the closed cell foam core – are presented below in Table 2-2 and Table 2-3.

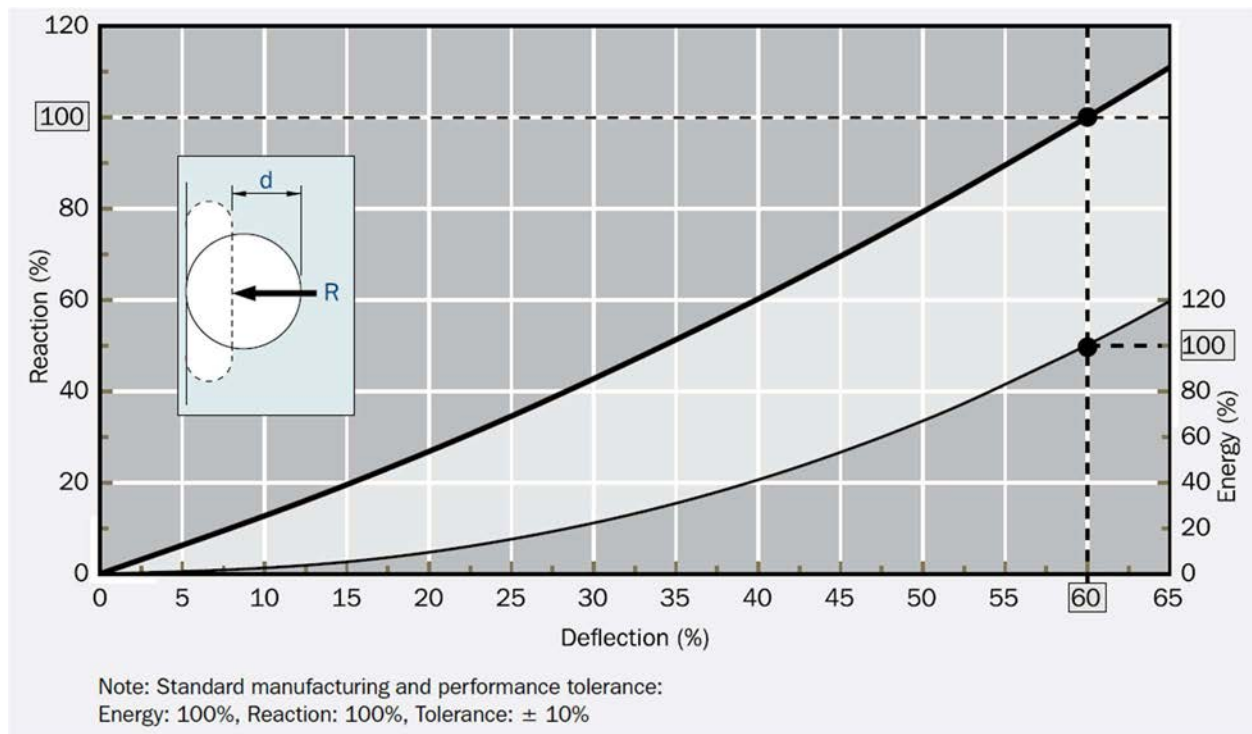


Figure 2-3. Generic plot for SeaGuard fender reaction and energy as a function of fender deflection. (Trelleborg Marine and Infrastructure, 2017)

Table 2-2. Trelleborg material properties for SeaGuard fender skin. (Trelleborg Marine Systems, 2018)

Sprayed Polyurethane Elastomer Skin	
Tensile Strength	1.38e7 Pa
Elongation	300%
Tear Strength	3.24e4 Pa

Table 2-3 Trelleborg material properties for SeaGuard fender core. (Trelleborg Marine Systems, 2016)

TMS Standard Energy Absorbing Foam	
Density	61.67 kg/m <sup>3</sup>
Tensile Strength	29.65e4 Pa
Compressive Strength at:	
10% Deflection	2.69e4 Pa
25% Deflection	4.76e4 Pa
40% Deflection	7.72e4 Pa
50% Deflection	10.96e4 Pa

Unfortunately, to model these materials in ANSYS, additional information was needed that was unavailable. As such, two generic replacement materials that were readily available in the ANSYS material library were used throughout this study to approximate the fenders' material characteristics. For the outer skin, a generic polyurethane rubber was used, with the material properties shown in Table 2-4.

Table 2-4. Model material properties for fender skin.

Rubber, Polyurethane	
Density	1200 kg/m <sup>3</sup>
Zero Thermal-Strain Reference Temperature	20 °C
Tensile Ultimate Strength	4.517e7 Pa
Tensile Yield Strength	4.517e7 Pa

For the foam inner core, a generic low-density polyethylene foam was used, with the material properties shown in Table 2-5.

Table 2-5. Model properties for fender core.

Foam, LDPE	
Density	32.94 kg/m <sup>3</sup>
Young's Modulus	8.485e5 Pa
Poisson's Ratio	0.199
Bulk Modulus	4.6982e5 Pa
Shear Modulus	3.5384e5 Pa
Isotropic Secant Coefficient of Thermal Expansion	0.0002045 1/ °C
Tensile Ultimate Strength	4.131e5 Pa
Tensile Yield Strength	19900 Pa

## 2.2.2 Ship and Caisson Properties

During modeling, the fenders were assumed to be squeezed between a generic “ship” that was approximated as a structural steel hyperrectangle and a generic “caisson” that was approximated as another hyperrectangle. Since the focus of this thesis was on fender (as opposed to ship) performance, this approach was deemed adequate. The generic “ship” was 14.37-ft long by 11-ft wide by 2-ft deep. Its material properties are shown below in Table 2-6:

Table 2-6. Model properties for ship hull.

Structural Steel	
Density	7850 kg/m <sup>3</sup>
Young's Modulus	2e11 Pa
Poisson's Ratio	0.3
Bulk Modulus	1.6667e11 Pa
Shear Modulus	7.6923e10 Pa
Isotropic Secant Coefficient of Thermal Expansion	1.2e-5 1/ °C
Compressive Yield Strength	2.5e8 Pa

Similarly, the generic caisson’s dimensions were 14.37 ft long by 11 ft wide by 2 ft deep. Its material was generic “concrete” from the ANSYS material library, since this



material is common in naval piers. The concrete's material properties are shown below in Table 2-7.

Table 2-7. Model properties for pier wall/caisson.

Concrete	
Density	2300 kg/m <sup>3</sup>
Young's Modulus	3e10 Pa
Poisson's Ratio	0.18
Bulk Modulus	1.5628e10 Pa
Shear Modulus	1.2712e10 Pa
Isotropic Secant Coefficient of Thermal Expansion	1.4e-5 1/ °C
Tensile Ultimate Strength	5e6 Pa

## 2.3 Boundary Conditions

As noted above, the modeled fenders were assumed to be squeezed between a generic “ship” and caisson.” This configuration is illustrated below in Fig. 2-4:

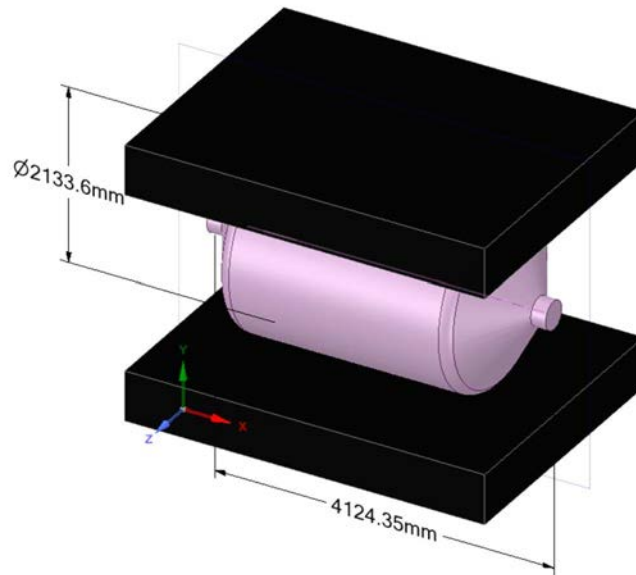


Figure 2-4. Isometric view of fender testing model, with fender width and radius. The pier/caisson was assumed to be fixed along one face as shown in Figure 2-5.

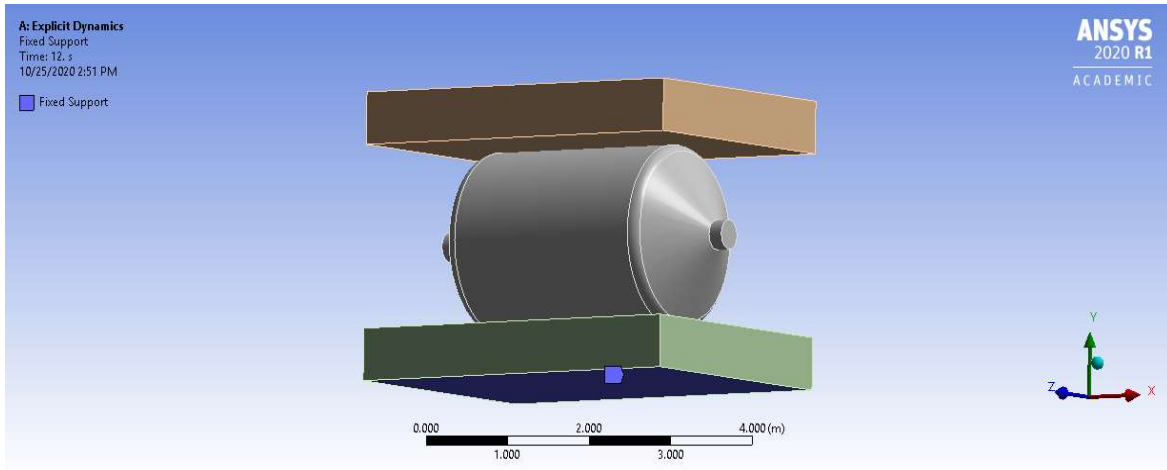


Figure 2-5. View of fender with fixed support on pier highlighted in blue.

Equations of motion associated with this fixity are as follows (ANSYS 2020):

$$\frac{dx}{dt} = 0 \quad (2-9)$$

$$\frac{dy}{dt} = 0 \quad (2-10)$$

$$\frac{dz}{dt} = 0 \quad (2-11)$$

Along the face of the generic “ship” furthest from the fender, velocities were applied as shown below in Fig. 2-6:

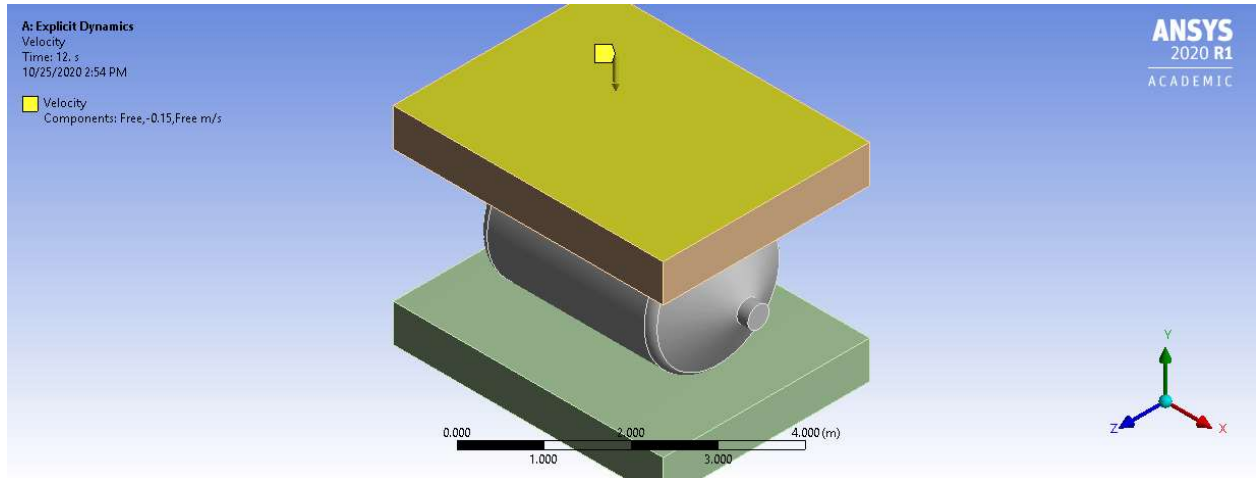


Figure 2-6. View of fender model testing model showing the ship face that has been given a velocity profile highlighted in yellow.

Equations of motion associated with this velocity distribution are as follows:

$$\frac{dx}{dt} = 0 \quad (2-12)$$

$$\frac{dy}{dt} = V_s \quad (2-13)$$

Or

$$\frac{dy}{dt} = V_c \quad (2-14)$$

$$\frac{dz}{dt} = 0 \quad (2-15)$$

where  $V_s$  is the static testing velocity and  $V_c$  is the cyclic testing velocity (please see below).

At first, investigators did not impose any boundary restrictions on the fender's movement. However, initial testing showed that if boundary restrictions were not imposed, the fender would tend to roll during loading/unloading. As such, two fixities (i.e., fixed supports) were imposed at each of the fender's endpoints. These fixities were intended to

mimic the practical application of the fender, where it is secured to the pier via an internal chain, as shown in Figure 1-5. During analysis, the forces on these fixed supports was measured and added to the force on the caisson to generate total forcing.

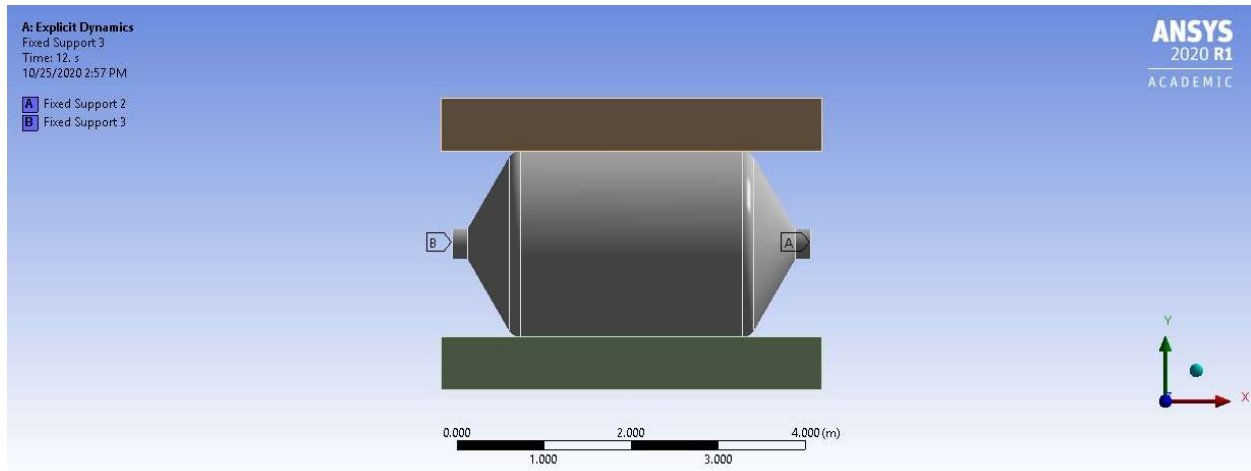


Figure 2-7. View of fender testing model showing the two fixities on the fender that have been given fixed supports, labeled “Fixed Support 2”, and “Fixed Support 3”.

The contact surfaces between the fender/pier; fender/ship; and polyurethane skin/foam core were treated as frictionless surfaces, although in future efforts this could easily be improved by adding a friction factor.

## 2.4 Mesh Characteristics

For this thesis, the mesh used had 22,493 nodes resulting in 72,117 unique elements across the three bodies. The mesh used on both the caisson and ship was a quadrilateral mesh, while the mesh used on the fender was a tetragonal mesh, as seen in figure 2-8.

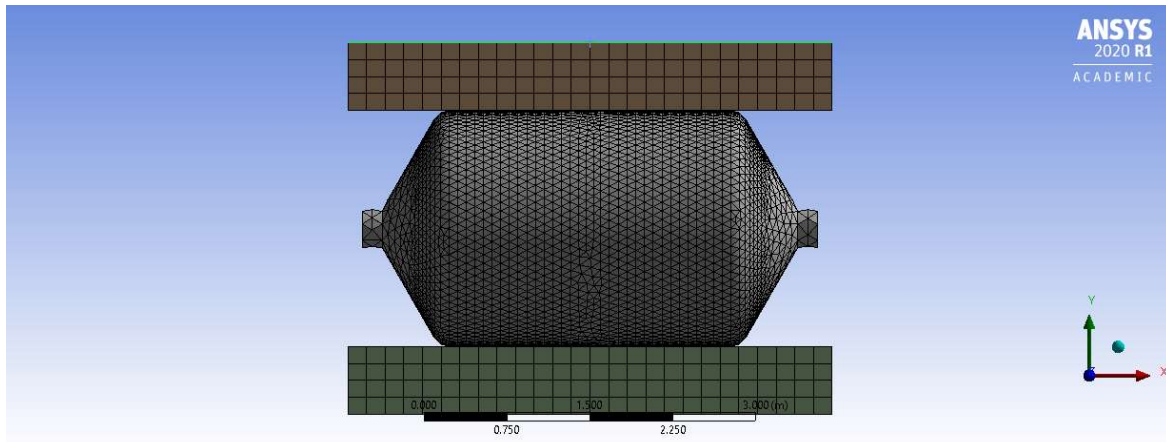


Figure 2-8. View of fender testing model with mesh visible.

The mesh used for the caisson and ship, was coarser than the fender mesh since the fender was the focus of this study. Using a coarser mesh on these lower interest elements decreased computational cost and led to faster runtimes. For explicit dynamics analysis, ANSYS (2020) recommends several mesh characteristics a uniformly sized mesh, with evenly sized elements because the explicit dynamics time step is controlled by the smallest mesh element. It is also important to note that the results of this study are directly correlated to the characteristics of the mesh used. In future work, it would be useful to conduct a mesh study to determine how/if different mesh geometries affect results.

## 2.5 Testing Methods

As implied above, two test-series were conducted – a quasi-static test-series and a dynamic test series. Details about these test-series are presented below:

### 2.5.1 Quasi-Static Testing

The purpose of the quasi-static test series was to mimic standard fender/deflection testing discussed in detail by ASTM F2192-05 (ASTM, 2017), whereby a fender is to be loaded using a load plate moving at a constant velocity until the fender

is deflected to approximately 60% of its original width. Trelleborg (2016) recommends that the loading rates should be no more than 0.0003 m/s. However, performing this sort of computational analysis would require a prohibitively small explicit timestep which would in turn lead to a model that could not feasibly be run within current time constraints using available computational resources. As such, an alternative testing matrix was developed using increasing velocities to determine if load rate significantly affected the shape of the force/deflection curve. The testing matrix is presented below in Table 2-8 and includes the total time required to achieve 60% deflections.

Table 2-8. Static testing velocity testing matrix

Test Number	Ship Velocity (m/s)	Testing Period (s)
1	0.0625	24
2	0.125	12
3	0.25	6
4	0.5	3
5	1	1.5
6	2	0.75

It is also important to note that while Trelleborg recommends a very slow load rate, the velocities of 0.0625, 0.125, are within the range shown in section 5.2 of ASTM F2192-05. The velocities of 0.5, 1, and 2 m/s are outside of this range. The purpose of these higher velocity simulations was to determine if the fender responded significantly differently to these faster load rates.

## 2.5.2 Cyclic Velocity Testing

After the completion of the quasi-static testing, cyclic testing of the fender was conducted. The fender model was subjected to two (2) impacts following a sinusoidal path, to mimic the impact of a wave on the ship, driving the ship into the fender. The velocity equation is shown in equation 2-17.

$$\frac{dy}{dt} = -V_0 \sin\left(\frac{2\pi}{T}t\right) \quad (2-17)$$

Where  $\frac{dy}{dt}$  is the instantaneous velocity,  $V_0$  is the input velocity,  $T$  is the wave period, and  $t$  is the time.

The impact velocities used were calculated using moored ship velocity data from UFC 4-152-01 (DoD, 2017), shown in Figure 2-9, and the published gross tonnage of a LCS, which is approximately 3,000 long tons (*SURFPAC Littoral Combat Ships Page*, n.d.). Using these data, an impact velocity for each mooring condition was calculated. These velocities were 0.334 m/s for an exposed berthing condition; 0.25 m/s for a moderate berthing condition; and 0.15 m/s for a sheltered berthing condition.

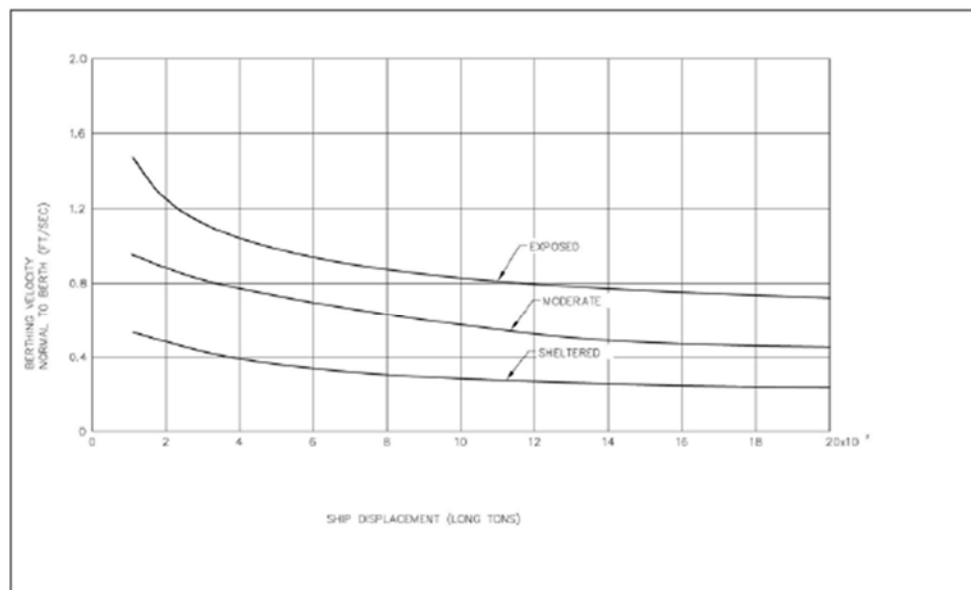


Figure 2-9. Plot of ship velocity as it pertains to ship weight and berthing conditions as seen in UFC 4-152-01 (DoD, 2017)

To test the impact of wave period on fender response, four different wave periods were chosen:  $T = 1.5, 3, 4.5$ , and 6 seconds. Using the calculated velocities and

chosen wave periods, a testing matrix was developed. This matrix is shown in Table 2-9, while A sample velocity profile is shown in Figure 2-10.

Table 2-9. Cyclic velocity testing matrix.

Test Number	Input Ship Velocity (m/s)	Wave Period (s)	Test Duration (s)
1	0.15	1.5	3
2	0.15	3	6
3	0.15	4.5	9
4	0.15	6	12
5	0.25	1.5	3
6	0.25	3	6
7	0.25	4.5	9
8	0.25	6	12
9	0.334	1.5	3
10	0.334	3	6
11	0.334	4.5	9
12	0.334	6	12

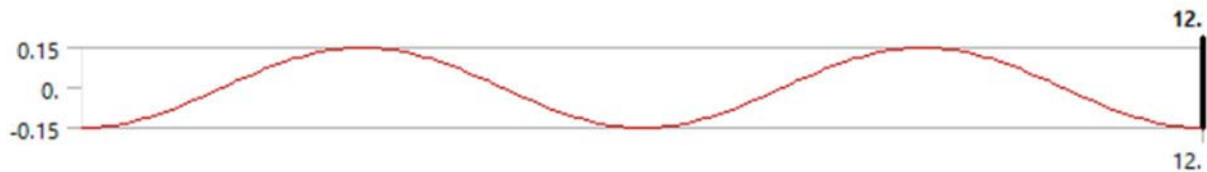


Figure 2-10. Example velocity profile for cyclic testing. X-axis has units of seconds, and Y-axis has units of m/s.

For each run, directional deflection of the fender body and force reactions at the two fixities and the main fender body were taken, in order to analyze the reaction vs deflection curve created.

In order to compare the analysis results to the published fender reaction data, the directional deformation of the fender body, in the x, y, and z directions. The force readings from the fender body, as well as the force readings from the two fixities were taken in the x, y, and z directions. These readings were then used to create three different plots.



## 2.6 Data Analysis

During each simulation, directional deformation of the fender body in the x, y, and z directions was tracked using two mechanisms. First, maximum deflection along the outside fender skin was saved directly in ANSYS. Secondly, projectile motion was used to find the “ship’s” position over time:

$$\delta = V_0 \Delta t \quad (2-18)$$

where  $\delta$  is the deflection;  $V_0$  is the ship speed; and  $\Delta t$  is the explicit timestep. These data were used to plot deflection versus time curves for each simulation.

Force was tracked by saving the reaction force on each models’ three fixities (behind the caisson; and on each ends of the fender) in the x, y, and z directions. Total force was computed by adding together each of these forces’ directional components. These data were used to develop force versus time curves.

Finally, force/deflection data were combined and used to plot several force/deflection curves. If different load rates (or load cycles, in the transient loading cases) led to different force/deflection curves – either in terms of their slopes, intercepts, or behavior (i.e., linear versus nonlinear), then this could mean that a dynamic response was invoked. If all curves were relatively similar, this would indicate that the simulations showed that the fenders responded similarly even when subjected to higher loading rates.

## CHAPTER 3 RESULTS

The testing matrices outlined in Tables 2-8 and 2-9 were completed according to the testing protocol outlined in Chapter 2. Each simulation was run until the test was completed, or the fender model failed under loading conditions. The results of these tests are illustrated in this chapter in several figures. In each of these figures, simulated deflection (blue line) and deflection computed from input velocity were plotted as a function of time (top); simulated force was plotted as a function of time (middle); and force was plotted as a function of displacement (bottom). Note that total force was computed by adding the forces on each of the fenders' end fixities with total force on the caisson's fixity. For cyclic results, these forces components were added to the plots as well to illustrate the relative contribution of each fixity on total fender force.

### **3.1 Quasi-Static Testing**

Data from quasi-static simulations are presented below in Fig. 3-1 through Fig. 3-6:

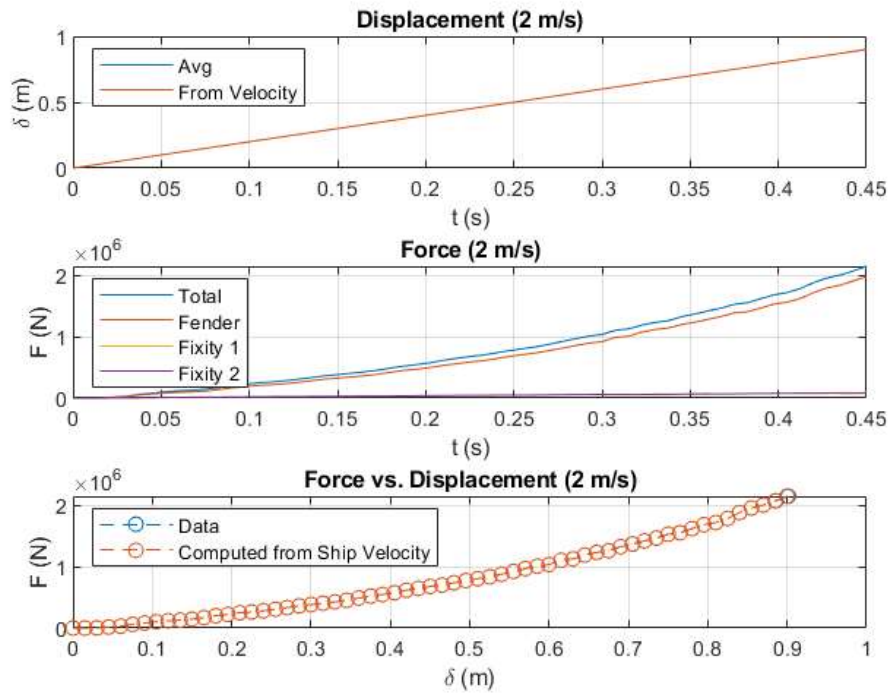


Figure 3-1. Quasi-static simulation with 2 m/s ship velocity results

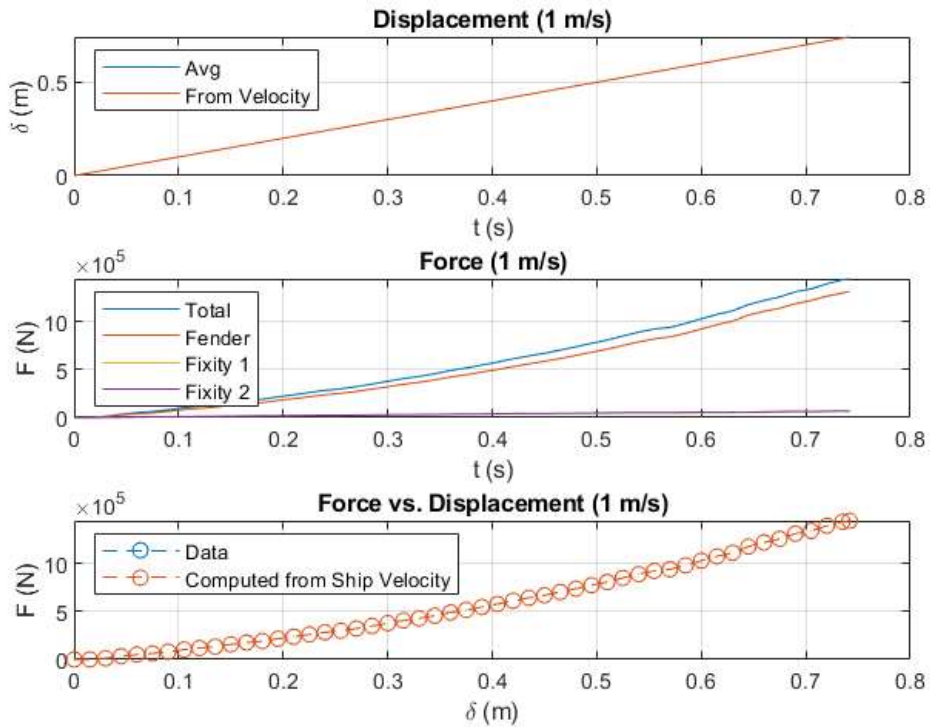


Figure 3-2. Quasi-static simulation with 1 m/s ship velocity results

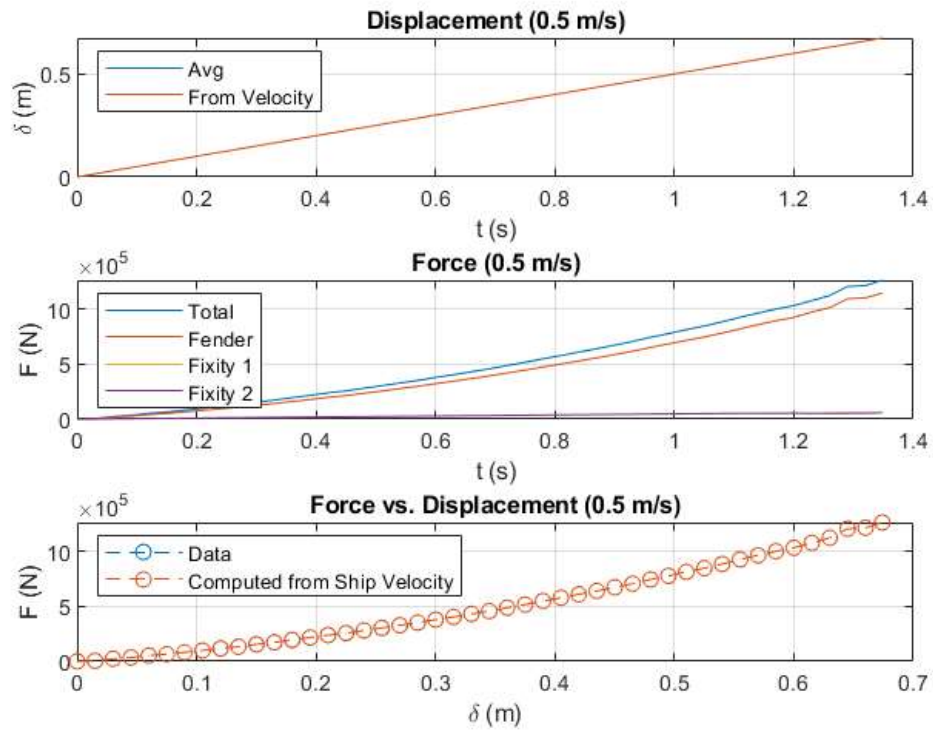


Figure 3-3. Quasi-Static simulation with 0.5 m/s ship velocity results

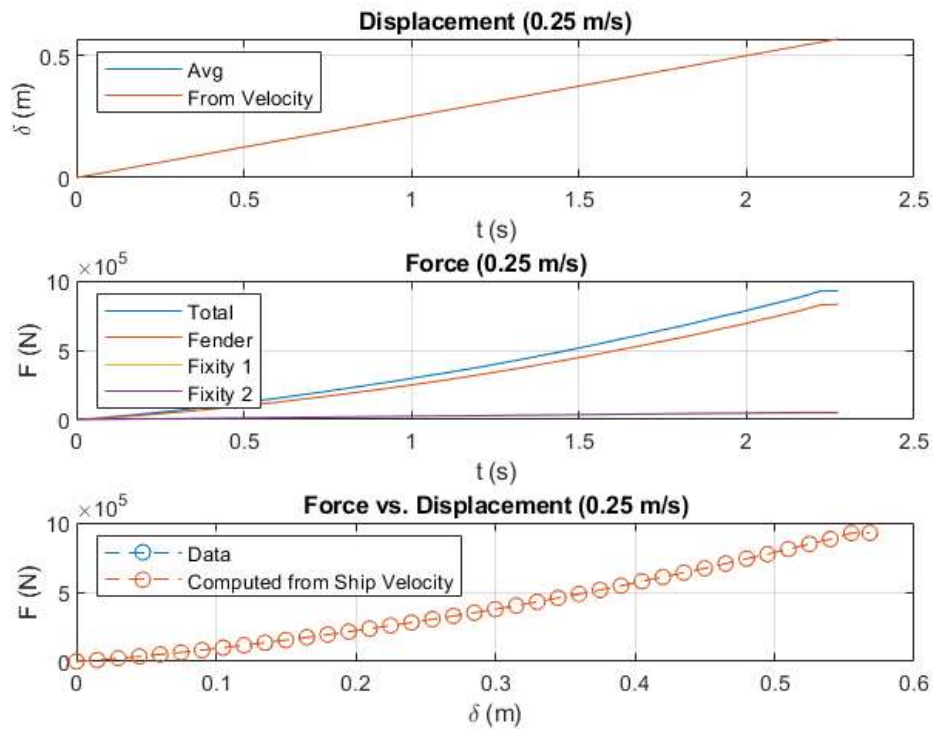


Figure 3-4. Quasi-static simulation with 0.25 m/s ship velocity results

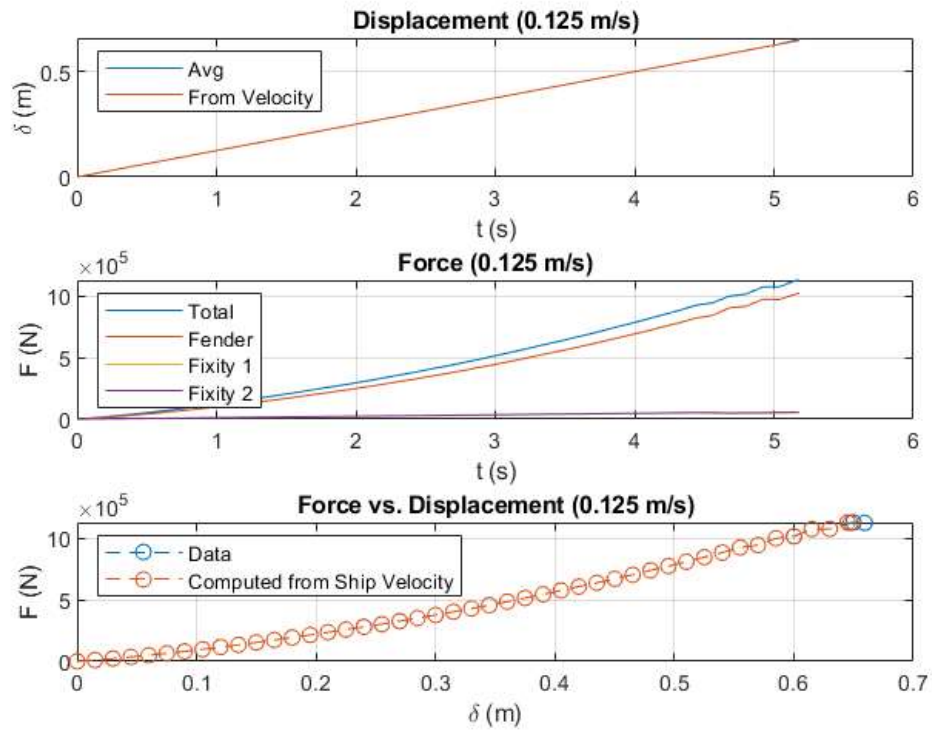


Figure 3-5. Quasi-static simulation with 0.125 m/s ship velocity results

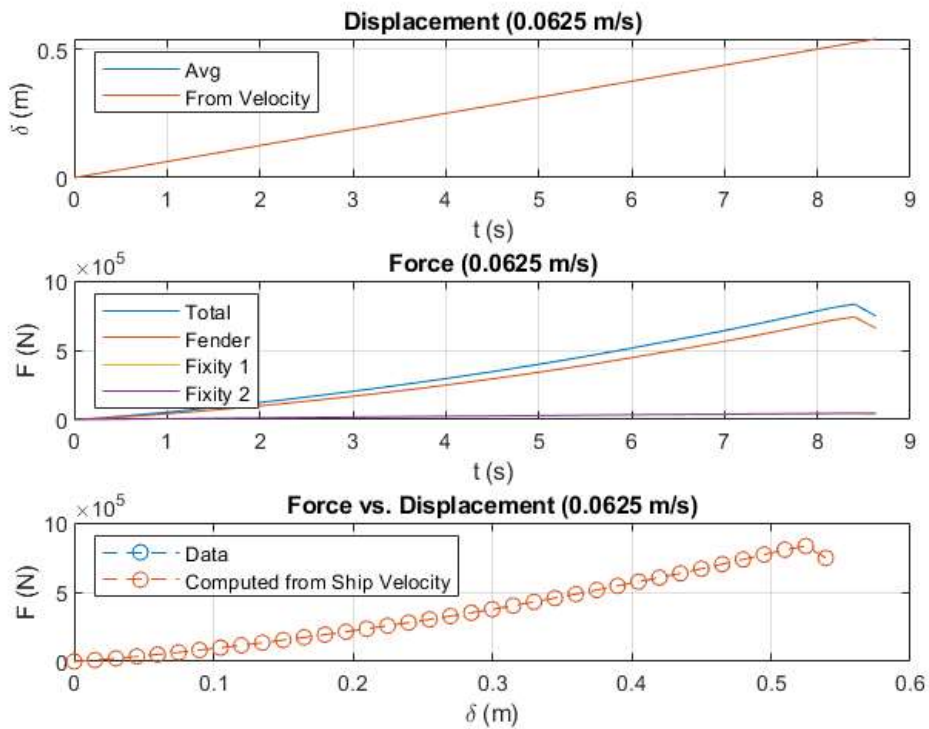


Figure 3-6. Quasi-static simulation with 0.0625 m/s ship velocity results

### 3.2 Cyclic Testing

Data from 1.0-s period testing are presented below in Fig. 3-7 through Fig. 3-18. These figures are grouped by wave period. As such, data from the 1.5-s period simulations are presented in Fig. 3-7 through Fig. 3-9. Data from the 3-s period simulations are presented in Fig. 3-10 through Fig. 3-12. Data from the 4.5-s period simulations are presented in Fig. Fig. 3-13 through Fig. 3-15. And finally, data from the 6-s period simulations are presented in Fig. 3-16 through Fig. 3-18:

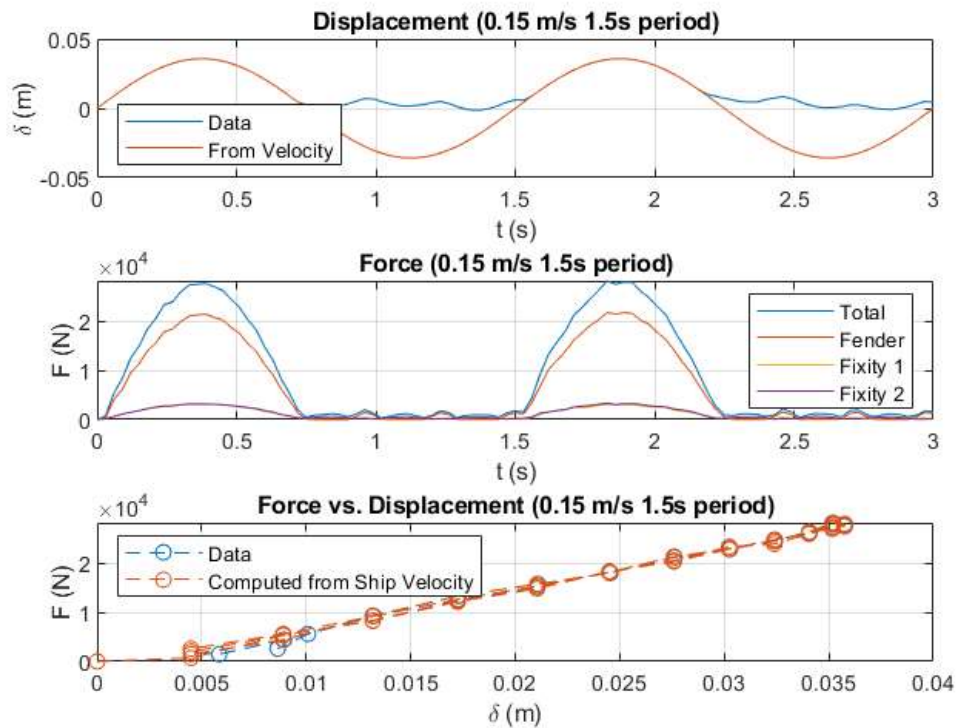


Figure 3-7. Cyclic test with 0.15 m/s ship velocity and 1.5 s period results

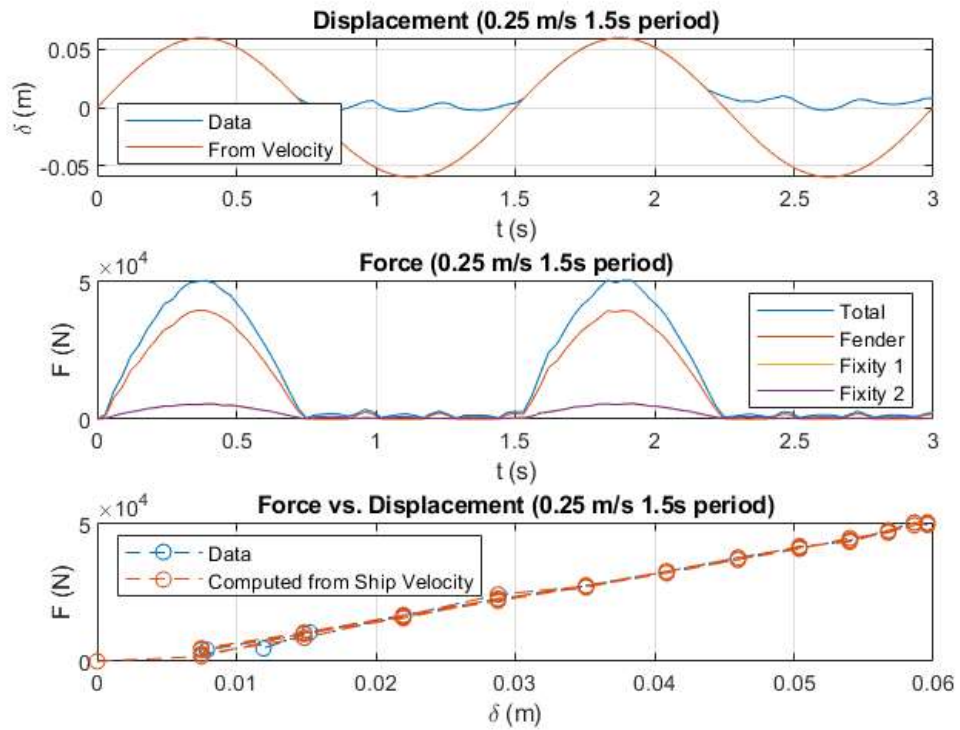


Figure 3-8. Cyclic test with 0.25 m/s ship velocity and 1.5 s period results

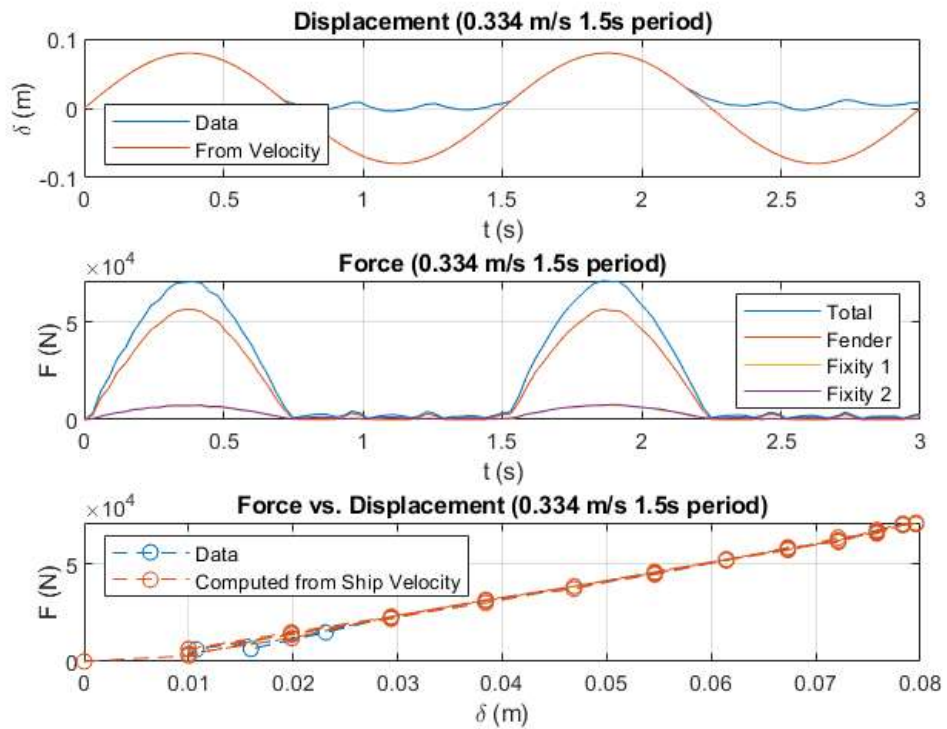


Figure 3-9. Cyclic test with 0.334 m/s ship velocity and 1.5 s period results



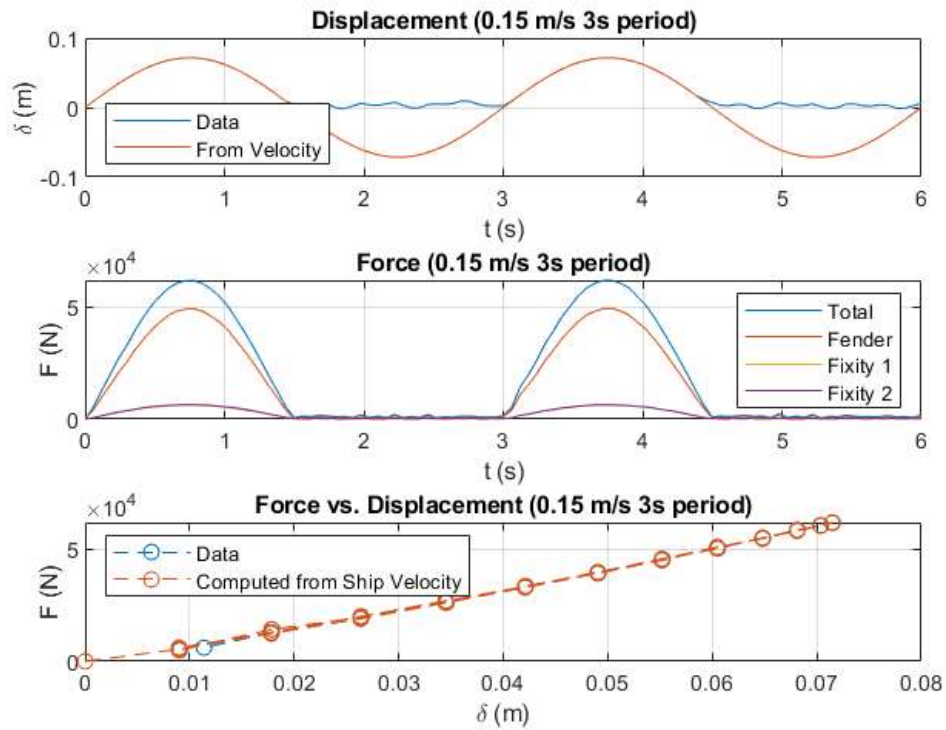


Figure 3-10. Cyclic test with 0.15 m/s ship velocity and 3 s period results

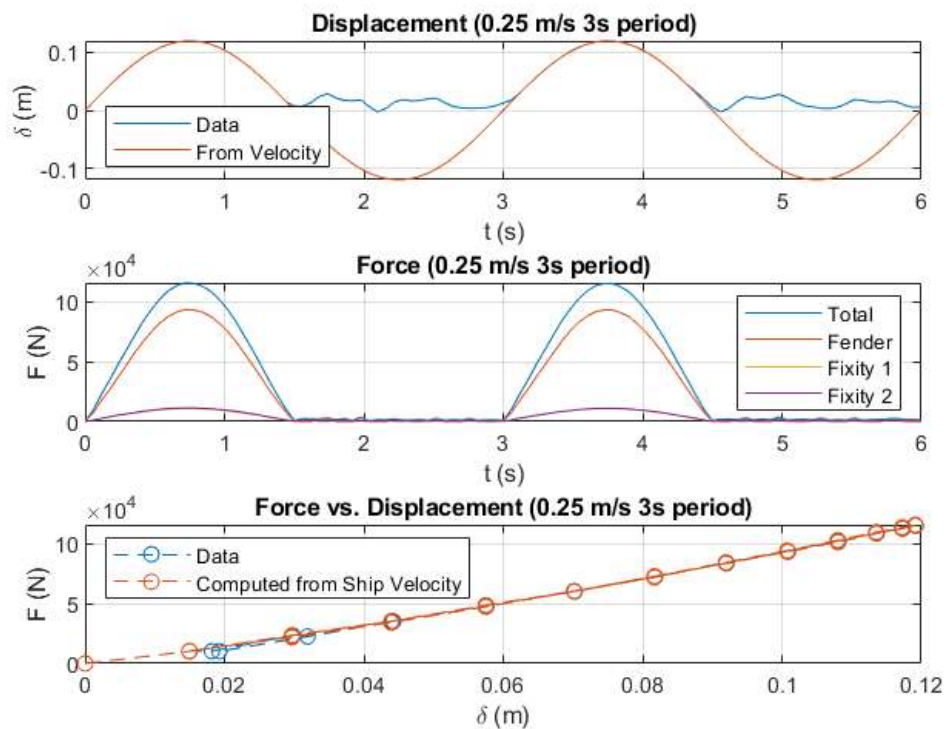


Figure 3-11. Cyclic test with 0.25 m/s ship velocity and 3 s period results



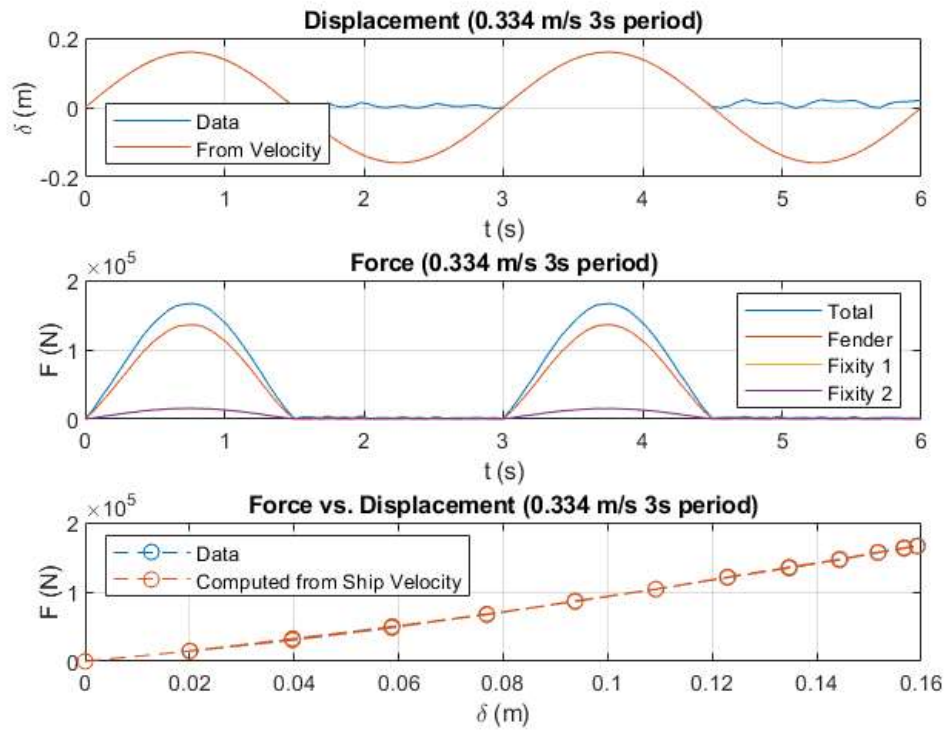


Figure 3-12. Cyclic test with 0.334 m/s ship velocity and 3 s period results

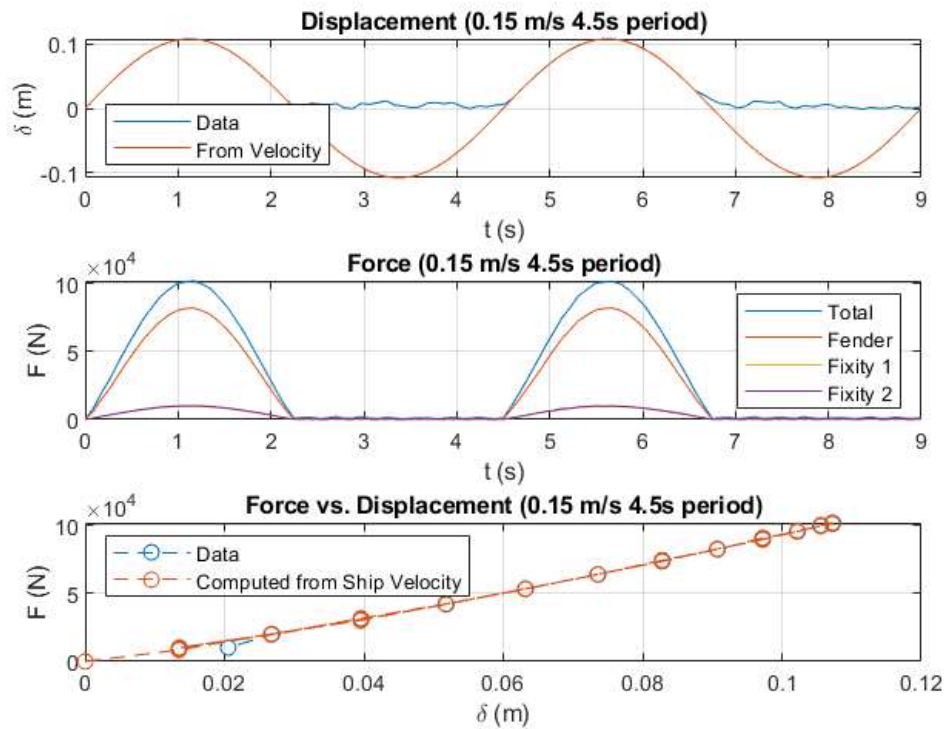


Figure 3-13. Cyclic test with 0.15 m/s ship velocity and 4.5 s period results

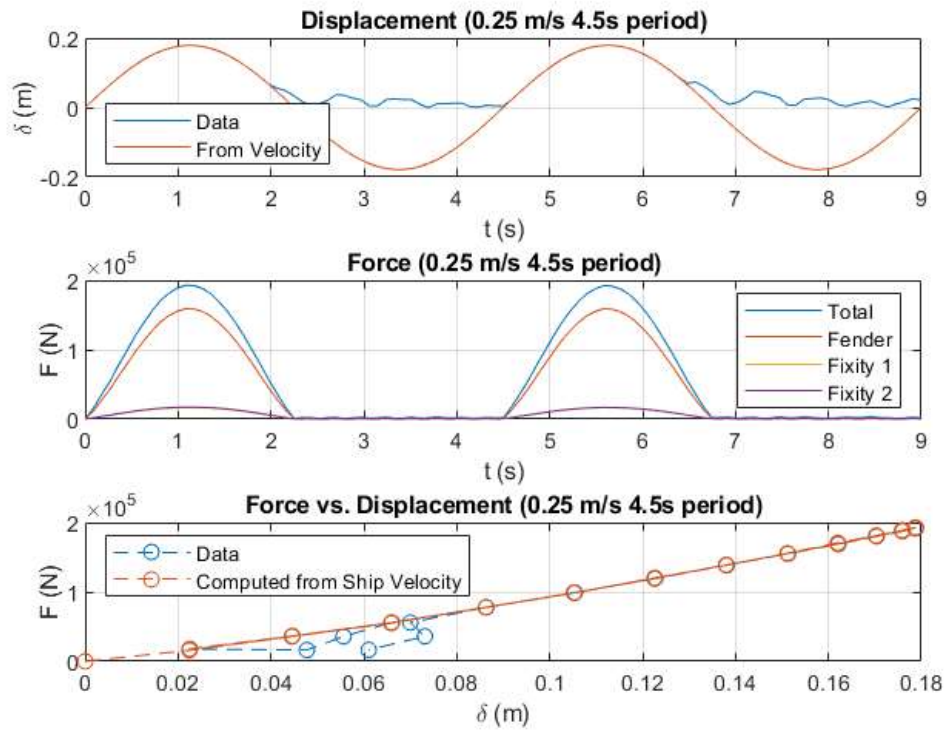


Figure 3-14. Cyclic test with 0.25 m/s ship velocity and 4.5 s period results

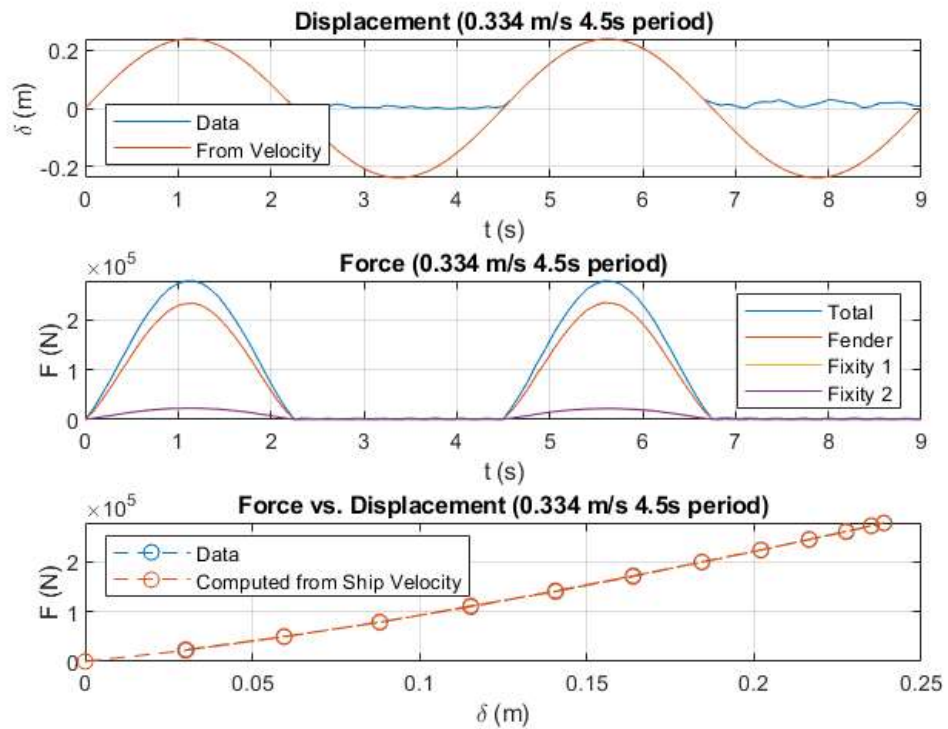


Figure 3-15. Cyclic test with 0.334 m/s ship velocity and 4.5 s period results.

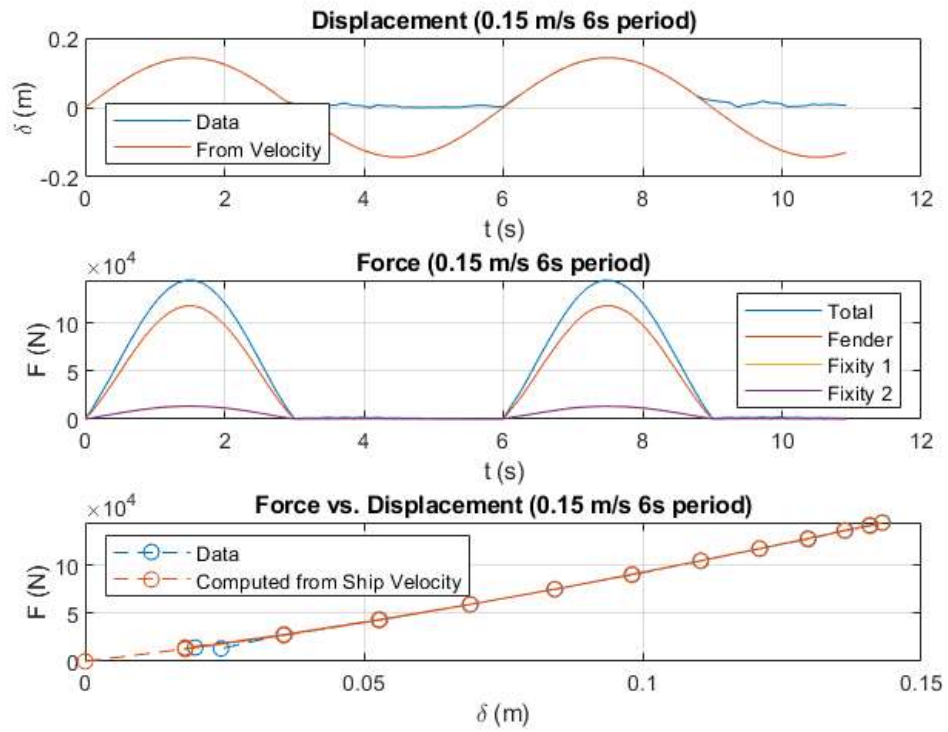


Figure 3-16. Cyclic test with 0.15 m/s ship velocity and 6 s period results

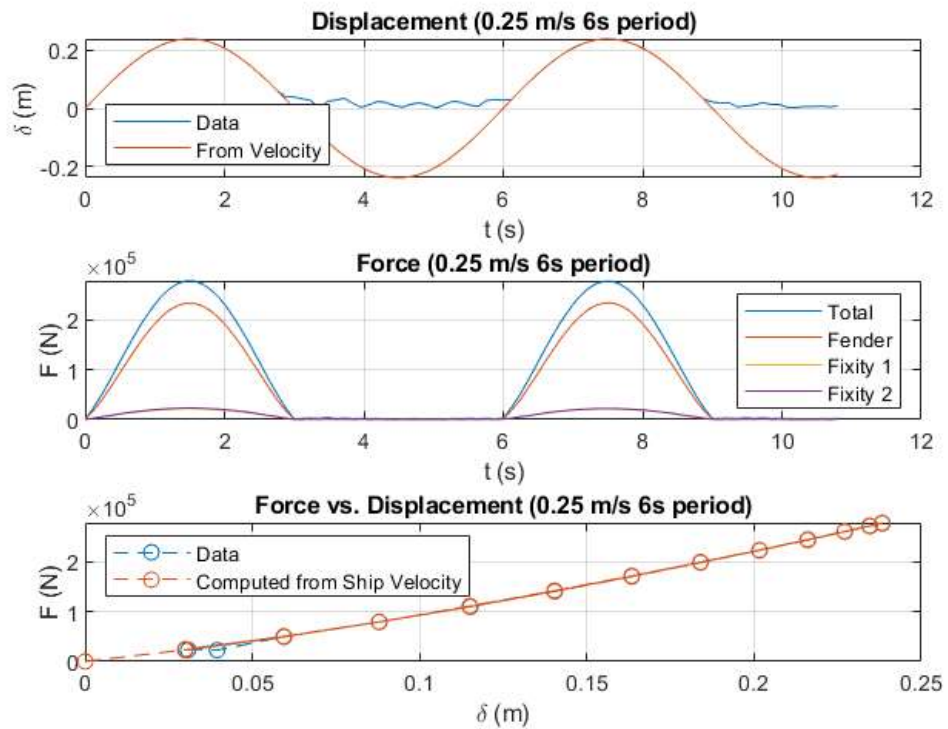


Figure 3-17. Cyclic test with 0.25 m/s ship velocity and 6 s period results

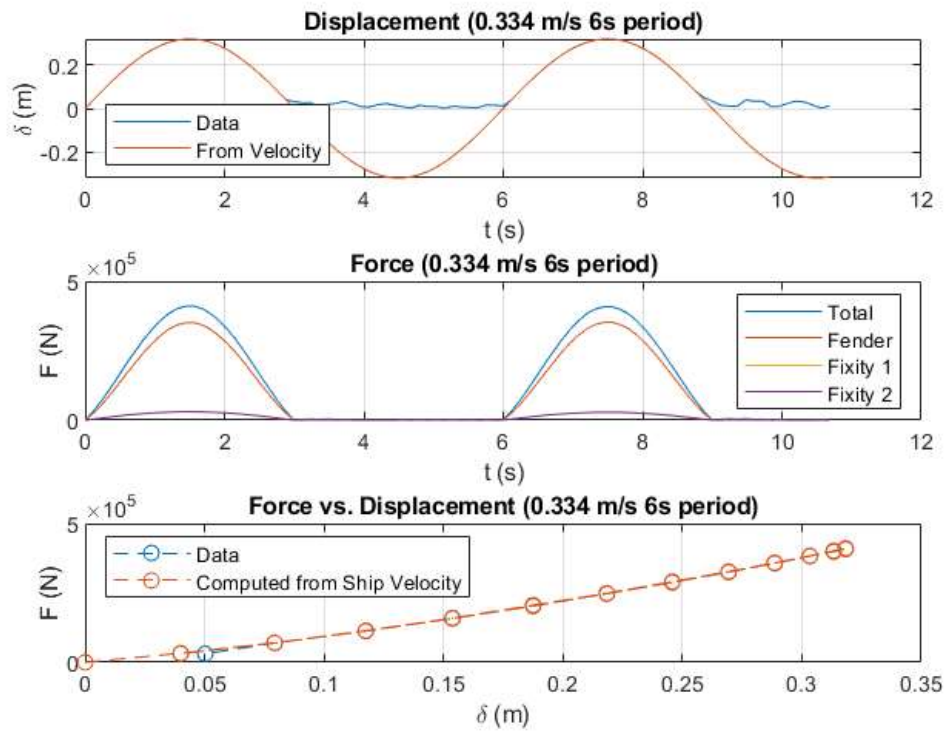


Figure 3-18. Cyclic test with 0.334 m/s ship velocity and 6 s period results

## CHAPTER 4 DISCUSSION

### 4.1 Quasi-Static Testing

The results of the quasi-static testing indicated that the speed of loading had little to no effect on the force response of the fender – at least throughout elastic deformation. A combined plot of the quasi-static simulations, along with a best-fit regression line through all data points is shown in Figure 4-1 to illustrate this:

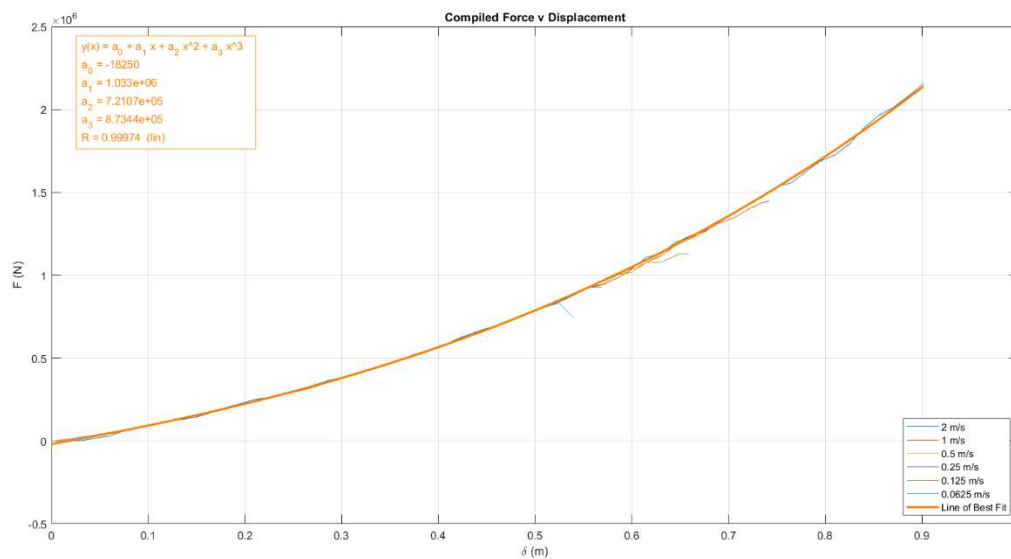


Figure 4-1. Plot of all quasi-static testing simulations with line of best fit and equation.

Unfortunately, due to the difference in materials used for the testing run, from the actual fender material, a direct comparison to the fender performance values given in Table 2-1 was not possible. However, a visual comparison to Figure 2-3, the generic reaction plot for SeaGuard fenders, showed that the fenders did not behave in a manner markedly different than that of the published data.

However, it was interesting to note that load rate appeared to affect fender failure. To illustrate this, percent maximum deflection at failure was plotted as a function

of load speed (Fig. 4-2). As shown, slower load speeds appeared to lead to faster failure as a function of deflection.

One possible explanation for this phenomenon could be that the fender is failing sooner at a slower loading velocity due to the increased amount of time that the fender is under load. This could be causing more stress to be placed on the fender, causing a failure sooner in the deflection profile than at a faster velocity. Physical testing will be needed to confirm this hypothesis.

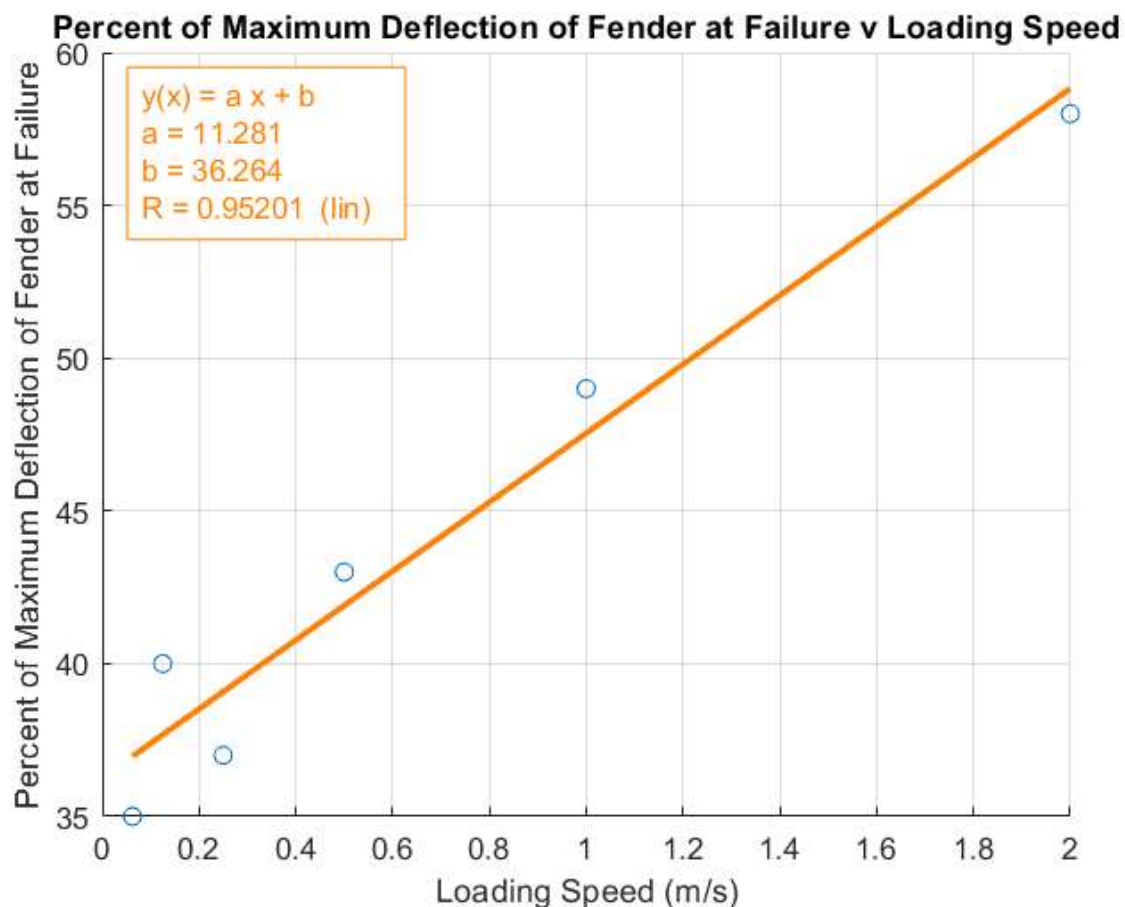


Figure 4-2. Plot of percent of maximum deflection of the fender at failure as a function of loading speed.

Preliminarily, it is believed that the inner core is failing at the endpoint fixities under a sort of quasi-fatigue loading. As such, continuously pressing against the foam causes

the foam matrix to fail over time. This is illustrated below in Fig. 4-3 which illustrates a fender at failure. Note that the inner core has significantly deflected.

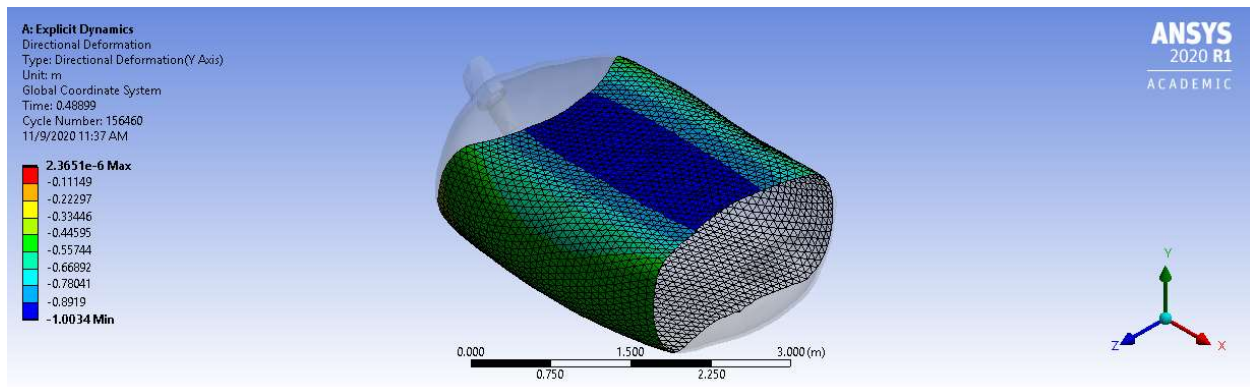


Figure 4-3. LDPE foam core of fender at failure during 2 m/s quasi-static testing.

Further investigation is needed to determine if this phenomenon is reflected in physical testing, as well as to determine the method of failure.

## 4.2 Cyclic Testing

Results from the cyclic testing indicated that there was not a significant difference in fender reactions under cyclic loading conditions when compared to quasi-static conditions. A combined plot of the cyclic simulations, along with a best-fit regression line through all data, is shown below in Figure 4-4 to illustrate this:



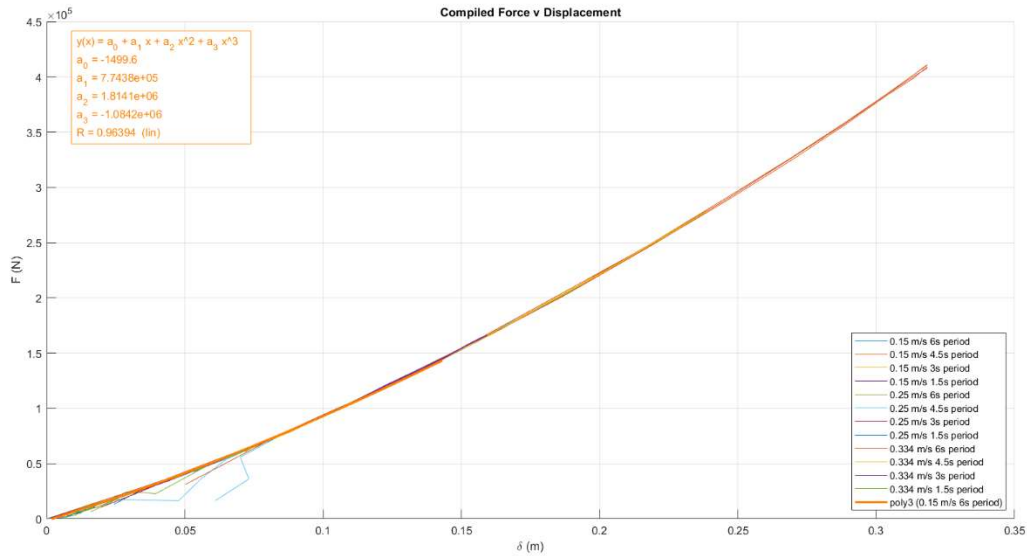


Figure 4-4. Plot of all cyclic testing simulations with line of best fit and equation.

It is also interesting to note that the cyclic testing did not have the same correlation between the loading speed and percentage of maximum deflection at failure of the fender. This is likely due to the fact that the fender compression in the cyclic testing models was at its maximum 0.32 m, which occurred during the 0.334 m/s velocity 6 s period simulation. Using the results shown in Figure 4-2, at this velocity, the fender would need to be compressed to 40.03% of its maximum rated deflection, which, for the fender simulated, is 0.60 m. From this, it can be concluded that the cyclic loading did not compress the fenders sufficiently to possibly induce material failure. This is an area for further study, but preliminarily it would appear to indicate that if anything, cyclic loading like the loading that would be seen during a HWM event would, if anything, actually help as opposed to cause ship damage.

### 4.3 Conclusions

The results of both the quasi-static testing and the cyclic testing appear to show that there is no significant difference in fender reaction from a cyclic loading pattern.



Figure 4-5 below shows both the combined plots of the cyclic tests and static tests, as well as their respective lines of best fit. The top of Fig. 4-5 is from cyclic loading; from the middle is quasi-static loading; and the bottom is the best-fit regression line from cyclic loading overlaid upon the best-fit regression line from quasi-static loading. As shown in the bottom plot, these lines were almost identical.

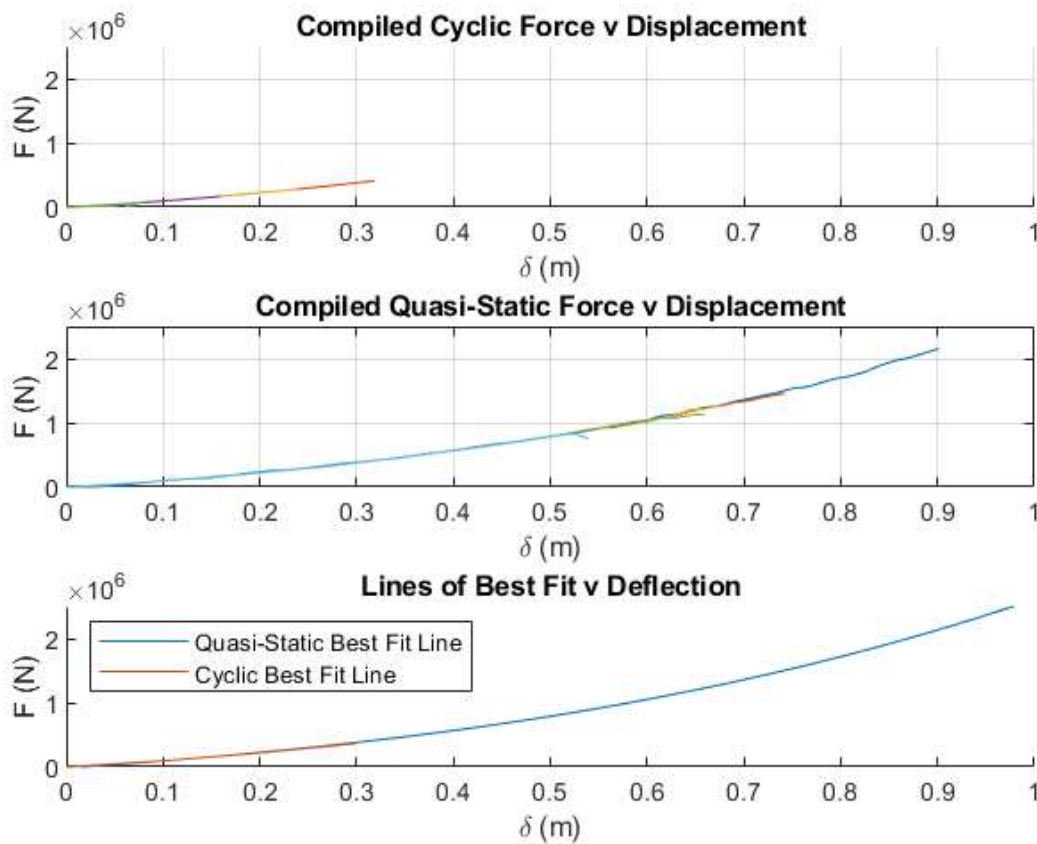


Figure 4-5. Compiled plots of both cyclic and quasi-static testing, along with their lines of best fit.

This point bears a bit of further discussion. The load sequence associated with cyclic loading is illustrated below in Fig. 4-6 through 4-8. Shown in these figures are the following:

1. At  $t = 0$ , the simulated ships started in contact with the fenders.

2. From  $t = 0$  to  $t = T/4$  ( $T$  is the wave period), the ships moved toward the fenders at a decreasing rate of speed and compressed the fenders.
3. From  $t = T/4$  to  $t = T/2$ , the ships moved away from the fender at an increasing rate of speed. During this time, the fenders returned to zero deformation.
4. From  $t = T/2$  to  $T = 3T/4$ , the ships continued to move away from the fenders at a decreasing rate of speed. This caused a space to form between the fenders and the ships.
5. From  $t = 3T/4$ , the ships began moving toward the ships once again. At  $t = T$ , the ship was back in contact with the fender, and the cycle could repeat.

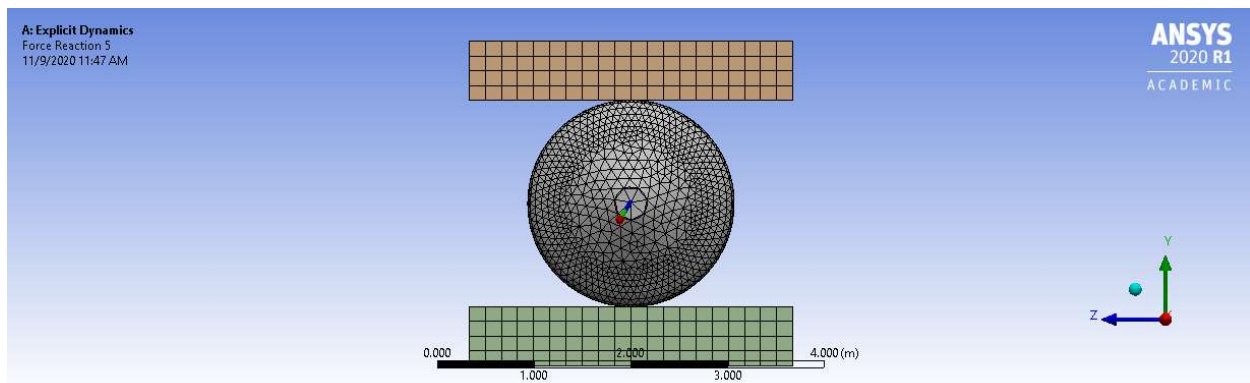


Figure 4-6. Starting position of cyclic testing simulation, with the ship model in contact with the fender model.

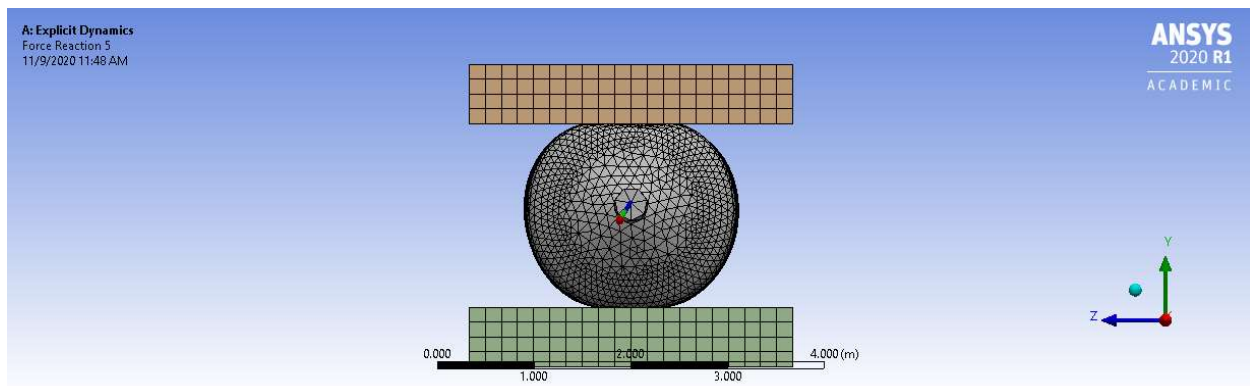


Figure 4-7. Cyclic testing simulation at time  $T/4$ , at full compression.

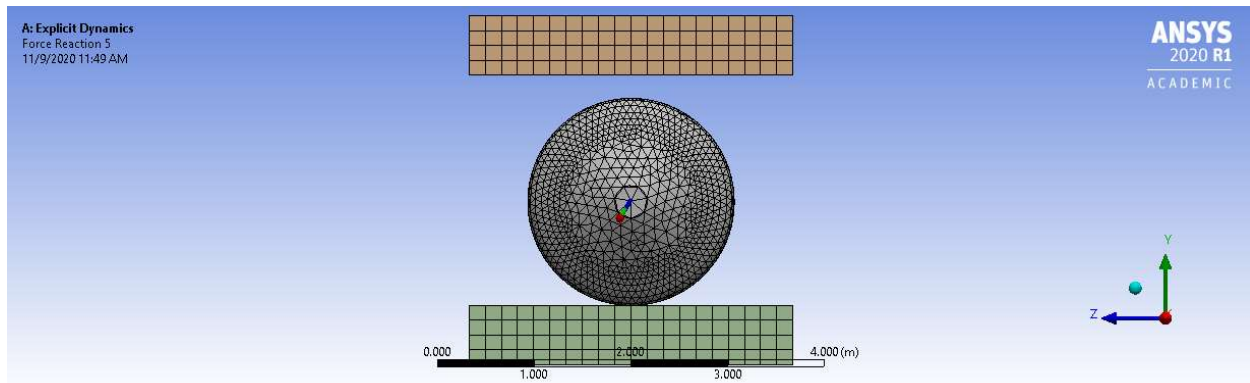


Figure 4-8. Cyclic testing simulation at time  $3T/4$ , at its farthest position from the fender.

It is especially interesting to note that the second cycle would have started with an impact load as the space between the fenders and the ships approached zero. This impact load appears to have had little effect on simulated fender performance because as seen in the data, the force/deflection relationships for the first simulated wave cycles were almost identical to the force/deflection relationships shown for the second simulated wave cycles. Future work in this subject should focus on confirming these behaviors using physical testing.

## CHAPTER 5

### SUMMARY, CONCLUSIONS AND DISCUSSION OF FUTURE WORK

To summarize, investigators were attempting to determine if cyclic loading of a SeaGuard marine fender would provoke a dynamic response. Two different sets of simulations were conducted to evaluate this. First, quasi-static testing that approximatlye replicated the testing method that would be used by the fender manufacturer, was conducted to determine the effects of loading speed on fender reaction. Secondly, cyclic testing was conducted to determine if repeated loading in a short time duration would provoke a dynamic response from the fender. Results showed the following.

- There was no impact on fender response provoked by a difference in loading speed during quasi-static testing.
- Cyclic loading of the fender did not provoke a dynamic fender response even under a second wave cycle where impact forcing could have caused different behavior.

In addition, correlations were developed between the loading velocity during quasi-static testing and the percent of fender maximum deflection at which it failed. Overall, results of this study lead to the conclusions that both loading speed and loading pattern do not have an impact on fender response. These results need to be validated using physical testing.

## LIST OF REFERENCES

- United States Department of Defense. (2020, September 3). *UFC 4-159-03 Moorings* . Whole Building Design Guide. <https://www.wbdg.org/ffc/dod/unified-facilities-criteria-ufc/ufc-4-159-03>.
- United States Department of Defense. (2017, January 24). *UFC 4-152-01 Design: Piers and Wharves* . Whole Building Design Guide. <https://www.wbdg.org/ffc/dod/unified-facilities-criteria-ufc/ufc-4-152-01>.
- NAVFAC Criteria Office, & Curfman, R. D., TR-6015-OCN Foam-Filled Fender Design to Prevent Hull Damage (1997). Port Hueneme, California; Naval Facilities Engineering Service Center.
- ASTM (2017). "Standard Test Method for Determining and Reporting Berthing Energy and Reaction of Marine Fenders", ASTM International West Conshohocken, Pa.
- Trelleborg Marine and Infrastructure. (2017). *Floating Fenders*. Trelleborg, Sweden; Trelleborg AB.
- Office of the Chief of Naval Operations, OPNAV INST 4700.7M Maintenance Policy for Navy Ships (2019). Washington , D.C.; Department of the Navy.
- Trelleborg Marine Systems. (2016). TMS Standard Energy Absorbing Foam: Minimum Properties.
- Trelleborg Marine Systems. (2018). *Sprayed Polyurethane Elastomer Skin: Minimum Mechanical Properties*.
- Trelleborg Marine Systems. (2018). *Standard SeaGuard Marine Fender*.
- SURFPAC Littoral Combat Ships Page*. (n.d.). United States Navy. Retrieved September 10, 2020, from <https://www.public.navy.mil/surfor/pages/LittoralCombatShips.aspx>

## BIOGRAPHICAL SKETCH

Zachary Eskew is a native of Park Ridge, Illinois. He graduated in 2015 from the United States Naval Academy with a Bachelor of Science in Mechanical Engineering and was commissioned as an Ensign in the United States Navy on May 22, 2015. His assignments include: Naval Mobile Construction Battalion ELEVEN, where he served multiple roles including Embark Officer, Facilities Engineering and Acquisition Division (FEAD) Marine Corps Logistics Base (MCLB) Albany, Georgia, where he served as a construction manager.

Zachary is a qualified Engineer in Training (EIT) in the State of Maryland. He was selected into the NAFAC Ocean Facilities Program in November of 2018 and has been a graduate student in the Master of Science in Civil/Coastal Engineering since August of 2019 at the University of North Florida.